Master of
Science Thesis
HT2020

# A comparison between LiF, $Al_2O_3$ and NaCl pellets for luminescence dosimetry based on clinical and laboratory measurements.

---


Edita Solak

Supervision

Christian Bernhardsson, Lovisa Waldner and Anniqa Rastbäck

This work has been performed at
the Medical Radiation Physics,Malmö and at SUS, Malmö

Department of Medical Radiation Physics,
Clinical Sciences, Lund
Lund University

# Contents

# Abstract

Radiation protection is of importance for the general public, patients and personnel in many different situations: rare accidents involving ionizing radiation, medical examinations or work tasks in the medical clinic or nuclear industry to name a few. Optimization in radiation protection and limitation of radiation doses are essential to prevent overexposure and for reducing negative health consequences. Therefore, research in the field of dosimetry is needed, to improve existing methods for dose monitoring and develop new ones. In luminescence dosimetry, thermoluminescence (TL) and optically stimulated luminescence (OSL) are examples of techniques used for quantifying radiation absorbed doses using passive dosemeters made from e.g. lithium fluoride (LiF) or carbon-doped aluminum oxide ($Al_2O_3$:C). OSL dosimetry studies are also conducted on newer materials. One such promising OSL material is household salt (NaCl) that has shown many beneficial dosimetric characteristics. Thus, it is of relevance to investigate whether household salt is a suitable choice for luminescence dosimetry, in relation to commercial alternatives.

The purpose of this project was to further investigate NaCl pellets as a potential passive personal dosemeter and specifically to compare NaCl pellets (OSL) to commercial detectors, such as LiF chips (TL) and $Al_2O_3$ discs (OSL). The three detector materials were positioned together in identical exposure geometries after which the absorbed doses to the various materials were estimated and compared. Possible effects due to differences in positioning, unit of calibration, and differences in energy dependence were taken into account. Both laboratory simulations and clinical experiments were conducted for the assessment of radiation doses in different nuclear medicine (NM) applications. These measurements were based on concerns and interests of staff members in the NM department, regarding the elution, preparation and handling of radiopharmaceuticals, the handling of patients, and radioactive waste. Experiments were carried out using radionuclides with photon energies relevant for the nuclear medicine clinic (140 keV and 662 keV).

The results presented in this project confirm previous results in terms of dose linearity and fading. Results show comparable dose estimations between the three types of detectors when studied under controlled conditions in the laboratory. For the experiments conducted in the clinic, the dose estimations show larger uncertainties compared to the laboratory simulations due to the low doses during the limited exposure times and consequently low signals in the various detector materials. Thus, the results for the $Al_2O_3$ discs during the preparation and elution of radiopharmaceuticals, as well as a couple other experiments were excluded as the signals appeared below detection limits.

To conclude, the obtained results provide dose estimations in reasonably good agreement between the three detector materials for a limited number of measurements, considering the energies involved and the duration of the measurements. Thus, NaCl has a strong potential to be utilized as an alternative point- and personal dosemeter. To improve the accuracy on the dose estimations, longer measurements are required in the clinic, and further measurements between NaCl and other commercial alternatives are necessary.

# Populärvetenskaplig sammanfattning

Det är viktigt att implementera strålskydd i olika situationer där allmänheten och patienter kan utsättas för joniserande strålning, bl.a. vid olyckor som involverar joniserande strålning, undersökningar i vården eller arbetsuppgifter i kliniken och kärnkraftverk. Optimering av strålskydd och begränsning av stråldoser är väsentligt för att motverka överexponeringar och för att reducera negativa hälsokonsekvenser. Det är därför viktigt att förbättra redan existerande metoder för dosövervakning och även utveckla nya. Termoluminiscens (TL) och optiskt stimulerande luminiscens (OSL) är exempel på tekniker som används för att kvantifiera stråldoser genom att använda passiva dosimetrar av bl.a. lithium fluorid (LiF) eller kol-dopad aluminiumoxid ($Al_2O_3$:C). Ett nytt lovande OSL material är hushållssalt (NaCl) som har många förmånliga dosimetriska egenskaper. För att undersöka om hushållssalt är ett lämpligt alternativ inom luminiscens dosimetri, i förhållande till kommersiella OSL/TL material, så är det viktigt att utföra en del jämförande studier.

Syftet med detta arbete är att ytterligare studera och jämföra saltets potential som en passiv person-dosimeter och jämföra det med kommersiella alternativ som LiF (TL) och $Al_2O_3$ (OSL). Alla tre material positionerades tillsammans i identiska exponeringsgeometrier, vartefter absorberad dos till de olika materialen uppskattades och jämfördes. Möjliga effekter p.g.a. skillnad i positionering, kalibrering och energiberoende beaktades. Simuleringar i labb och mätningar i kliniken genomfördes för uppskattning av stråldoser i olika nuklearmedicinska applikationer. Dessa mätningar baserades på den nuklearmedicinska personalens egna frågeställningar, gällande eluering, beredning och hantering av radiofarmaka, samt hantering av patienter och radioaktivt avfall. Experiment genomfördes med radionuklider med fotonenergier relevanta inom nuklearmedicin (140 keV och 662 keV).

Resultaten som presenteras i detta arbete bekräftar föregående resultat gällande dos-linjäritet och signalstabilitet. Resultaten visar jämförbara dosuppskattningar mellan de tre olika detektortyperna när de studerades under kontrollerade villkor i labbet. För experiment som utfördes i kliniken så visade dosuppskattningarna större osäkerheter jämfört med simuleringar i labbet. Detta p.g.a. låga doser under begränsade exponeringstider och därmed låga signaler i de olika detektormaterialen. Därmed blev resultaten för $Al_2O_3$ vid beredning och eluering av radiofarmaka, samt vid andra mätningar exkluderade, då signalerna låg under detektionsgränserna.

Avslutningsvis visar dosuppskattningarna god överensstämmelse mellan de tre detektormaterialen, vid flera mätningar, med hänsyn till energiberoende och korta exponeringstider. Saltet har en stor potential att utvecklas och användas som en alternativ punkt- och persondosimeter. För att öka noggrannheten i dosuppskattningarna krävs längre mätningar i den medicinska kliniken och ytterligare mätningar mellan saltet och andra kommersiella alternativ.

# List of abbreviations

| | |
|---|---|
| $Al_2O_3$ | Aluminium oxide |
| CW-OSL | Continuous wave optically stimulated luminescence |
| DASH | Detection and stimulation head |
| EPD | Electronic personal dosemeter |
| IR | Infrared |
| LAF | Laminar Flow Cabinet |
| LED | Light emitting diode |
| LiF | Lithium fluoride |
| LM-OSL | Linearly modulated OSL |
| MDD | Minimum detectable dose |
| MMD | Minimum measurable dose |
| NaCl | Sodium Chloride |
| NM | Nuclear medicine |
| OSL | Optically stimulated luminescence |
| PET | Positron Emission Tomography |
| PMMA | Polymethyl methacrylate |
| PMT | Photomultiplier tube |
| POSL | Pulsed OSL |
| SD | Standard deviation |
| SSM | Swedish Radiation Safety Authority |
| TL | Thermoluminescence |

# 1. Introduction

With an emphasis on radiation protection, dosemeters are essential tools used for the assessment of radiation dose during or after exposure to ionizing radiation. To ensure the safety of the general public during emergencies involving radioactive material, patients during medical examinations and staff during occupational exposures, dose-monitoring tools are indispensable. Therefore, new methods for optimizing the practices and related equipment used for dose assessments are constantly under development.

Currently, TL- and OSL-techniques are utilized in personal, clinical and environmental dosimetry. During the 1950s, LiF and $Al_2O_3$ gained popularity as detector materials used for TL due to their favorable dosimetric characteristics. Since then, new studies have determined that $Al_2O_3$ is more suitable for OSL dosimetry (Bøtter-Jensen, 2000; Bos, 2001). The commercial TLD- and OSLDs are sold and used worldwide under different names and in various forms, depending on the manufacturer and application.

Much attention has been drawn to research conducted in retrospective and prospective dosimetry, regarding the use of household salt (NaCl) as a potential dosemeter. Retrospective dosimetry utilizes materials that can be found around sites where incidents involving radioactive material have occurred. Both biological (e.g. blood) and physical (e.g. ceramics) materials can be used (Thomsen, 2004). In terms of physical retrospective OSL dosimetry, household salt (NaCl) has been particularly identified as a sensitive dosemeter material (Bernhardsson et al, 2009; Christiansson, 2014). In recent years, the use of NaCl as a detector material in prospective dosimetry has emerged, thereby extending its possibilities within dosimetry (Waldner et al, 2018; Waldner et al, 2020).

There are several personnel categories that are occupationally exposed to ionizing radiation. Among hospital staff, such as nuclear medicine (NM), the staff members are required to handle and prepare radiopharmaceuticals on a daily basis. The finger doses are regularly measured, as well as the overall monthly whole body dose. However, there are plenty of tasks where the occupational exposure is harder to measure and evaluate.

The general aim of this master thesis is to further investigate the potential use of NaCl pellets as a passive OSL dosemeter and more specifically to:

- Compare the NaCl pellets with commercially available passive dosemeters of LiF and $Al_2O_3$ in different types of exposure scenarios.

- To study performance of passive dosemeters in radiation protection areas of the NM department:

    1. The handling of radioactive waste.

2. The handling and preparation of radiopharmaceuticals during elution and preparation of radiopharmaceuticals.

3. The handling of patients post radiopharmaceutical injection.

# 2. Theory

## 2.1 Luminescence

Luminescence is a phenomenon which may occur in solid materials with crystalline structures. In such luminescent materials, energy is absorbed when the material is exposed to ionizing radiation. The absorbed energy can be stored during long periods of time and then converted to luminescence photons by stimulating the material by different means. Common methods for dosimetric materials are either thermal or optical stimulation (Bøtter-Jensen, 2000; Thomsen, 2004; Yukihara and McKeever, 2011). Therefore, the characteristics of luminescent materials makes them suitable for dosimetric purposes.

The crystal lattice in luminescent materials consists of arranged atoms and molecules. Due to the close proximity between the atoms and their orbitals, the electromagnetic forces cause the formation of energy bands with several energy states. The lower energy band, the valence band, is mostly occupied with tightly bound electrons in the ground state, whereas the upper energy band, the conduction band, has close to no electrons. Between the two energy bands is a space where (in a perfect crystal lattice) no electrons are allowed, that is the forbidden band gap. The electrons in the valence band require energy which exceeds the energy of the band gap, i.e. the energy difference between the conduction band and valence band, so that the electrons can break free and excite to the conduction band. Based on the size of the band gap, the materials are divided into three categories: conductor, insulator and semiconductor.

In a perfect crystal, excited electrons can roam freely through the conduction band until they lose all their energy and de-excite. However, most crystal structures are imperfect and contain numerous types of defects, which introduces energy states in the forbidden band gap. The defects can be divided in different categories, depending on what type of defect it is: vacancies, interstitials and impurities are common examples. In an imperfect crystal, electrons which are about to de-excite to the lower energy band, may get trapped at energy levels in the forbidden band gap, known as trap centers. The depth varies between trap centers and the energy from lattice vibrations may be sufficient to release electrons from shallow traps while deeper traps require more energy. The de-excited electrons that are trapped may enter a latency period that allow the stored signals to accumulate and to be stored for long periods of time before readout. Adding energy to the system releases the electric charges, re-exciting them to the conduction band. While losing their energy, the electrons may de-excite to a recombination center where it recombines with a hole. A luminescence photon is emitted when the recombination center de-excites.

### 2.1.1 TL vs OSL

Thermoluminescence (TL) and optically stimulated luminescence (OSL) are the two most common techniques used for luminescence dosimetry. They follow the same physical principles; releasing the electrons from trap centers by different means of stimulation according to a material dependent readout protocol. With TL the material is heated with increasing temperatures and as a temperature matches the energy of a trap, electrons are released. The amount of trapped electrons is proportional to the magnitude of exposure to ionizing radiation. Hence, the signal will be proportional to the magnitude of the absorbed dose.

In contrast, OSL is based on optical stimulation. As the name implies, optical tools such as light emitting diodes (LED), can be used to stimulate luminescence by choosing appropriate wavelengths and power during readout. Shortly after exposure to light, the OSL signal will reduce until the signal has been depleted. There are different modes of optical stimulation that can be used to measure the luminescence, continuous-wave OSL (CW-OSL), linearly modulated OSL (LM-OSL) and pulsed OSL (POSL). In the present work, CW-OSL is used, in which the samples are stimulated with a constant light intensity (Thomsen, 2004; Yukihara and McKeever, 2011).

The advantages and disadvantages of TL and OSL have been previously discussed, for example in a debate (McKeever and Moscovitch, 2003). One potential disadvantage with TL is the non-homogenous heating of the material, which means it is not certain that the TL material has been heated evenly or that all of the traps have been depleted. This affects the accuracy of the signal readout. Stimulation with heat consequently limits the number of luminescent materials that can be used with TL, as the crystal structures can be susceptible to heat induced alterations which may lead to destruction or even burning of the material. Before each reuse, TL-materials that are used for research purposes have to be annealed between 10 minutes to 2 hours depending on the material. This is often based on the manufacturer instructions (i.e. TLD Poland, 2001-2005). The TL-material also requires frequent calibration, especially if it has not been used continuously or if it has been damaged. Another disadvantage is depletion of the signal after a single readout. The advantage with TL is that it is a well-established method and that the materials can be exposed during daylight. In comparison to TL, OSL materials have to be kept in darkness during and after exposure to ionizing radiation as the signal will otherwise be depleted. Optical stimulation is also considered an advantage as it is a more suitable option for many materials since the samples can be read at room temperature. Also, it is possible to do repeated measurements on the same OSL dosemeter (Bøtter-Jensen, 2000; McKeever and Moscovitch, 2003).

## 2.2 Detector materials

Detector materials appropriate for luminescence dosimetry come in all shapes and sizes: grains, single crystals, chips, pellets, discs, powder, rods etc. A detector material is determined suitable when it possesses certain qualities essential in luminescence dosimetry, such as high radiation sensitivity, signal to dose linearity, low fading and tissue equivalence.

Detector materials with high radiation sensitivity provide higher signals at readout, which are used to estimate the absorbed doses. A linear signal to dose response is advantageous as it ensures correct dose estimation without using complex response curves. Likewise, it is preferable that the signal remains stable over time and does not fade. Materials with an effective atomic number, $Z_{eff,}$ close to that of soft tissue ($Z_{eff}$ = 7.65) are called tissue equivalent. Tissue equivalence means that the energy response of a material relative to tissue is the same. Thus, interaction between tissue equivalent detector materials and ionizing radiation may resemble how tissue would interact with the ionizing radiation, thereby it is a valuable tool in personal dosimetry (Bos, 2001; Kortov, 2007; Vargas and Vanhavere, 2011; Yukihara and McKeever, 2011; Geber-Bergstrand, 2017).

### 2.2.1 LiF

Lithium fluoride (LiF) is a widely used luminescent material. The luminescent properties of LiF were first investigated during the 1950s (Poston, 2003). Since then, impurities have been added to achieve better characteristics and today the two dominant forms of LiF are LiF:Mg,Ti and LiF:Mg,Cu,P. The former type was developed by Harshaw and is also referred to as TLD-100 (Poston, 2003), whereas the latter was described by Nakajima et al, 1978. Today, both types of LiF are manufactured in various forms and sold commercially by different companies. In comparison to LiF:Mg, Ti (TLD-100), LiF:Mg, Cu, P has shown better characteristics and a radiation sensitivity that is 20x higher. Throughout years of research, the sensitivity of LiF:Mg, Cu, P has been improved so that there is close to no residual signal after readout and annealing. Also, LiF has low fading and a close to tissue equivalent effective atomic number at $Z_{eff}$ = 8.3. The energy response for lower photon energies differs between the two forms of LiF, in which TLD-100 has shown an over-response, whereas LiF:Mg, Cu, P has shown an under-response (Ben-Shachar et al, 1999; Bos, 2001). A third option, which is rather tissue equivalent ($Z_{eff}$ = 7.3) and has better energy response is $Li_2B_4O_7$ (Bos, 2001).

### 2.2.2 $Al_2O_3$

Aluminium oxide ($Al_2O_3$) is a chemical compound that can be found in crystalline form. It is often referred to as corundum (Bos, 2001). During the 1990s, carbon-doped $Al_2O_3$:C, became widely used as a TL-material due to a high concentration of trap centers, thereby increasing the luminescent intensity (Akselrod et al, 1990; Vargas and Vanhavere, 2011). It has an effective atomic number that is higher than soft tissue, at $Z_{eff}$ = 11.3, and a TL radiation sensitivity that is 40-60x higher than TLD-100 (Bos, 2001; Yukihara and McKeever, 2011).

Due to its light sensitivity and thermal quenching effects that led to a decrease in efficiency (Bøtter-Jensen, 2000), $Al_2O_3$:C was determined to be more appropriate as a OSL-material. A linear dose response was observed for $Al_2O_3$:C, as a OSL-material, over an energy range between $10^{-4}$ -10 Gy and low fading less than 5% per year (Pradhan et al, 2008; Yukihara and McKeever, 2011). $Al_2O_3$:C are often produced as single crystals and used as commercial OSLDs manufactured by Landauer Inc.

### 2.2.3 NaCl

Household salt, chemically referred to as sodium chloride (NaCl), is a compound found in most households. Previous studies in retrospective (Bernhardsson et al, 2009; Christiansson, 2014) and prospective dosimetry (Ekendahl et al, 2016; Waldner and Bernhardsson, 2018; Waldner et al, 2020) have shown that NaCl, has dosimetric properties which can be optimized and used as a potential passive dosemeter. The studies have been made for both NaCl grains and NaCl pellets. Moreover, its availability and cost-effectiveness are an advantage compared to more expensive and less available options like LiF and $Al_2O_3$.

NaCl has a rather high effective atomic ($Z_{eff}$ = 15.2), meaning it is not tissue-equivalent. However, it shows a higher sensitivity to energies lower than 400 keV compared to soft tissue (Christiansson et al, 2018). Research has shown that NaCl pellets have a linear dose response up to at least 300 mGy (Waldner and Bernhardsson, 2018).

## 2.3 Dosimetric properties

Linearity between signal intensity and absorbed dose is one of the main general characteristics which are sought-after in dosimetric systems. Dose response curves are studied to investigate the linearity. The amount of and depth of the traps vary among different materials and are often the reason for a non-linear behavior. However, this usually occurs for higher doses, whereas the lower dose-range usually shows a more linear relationship (Yukihara and McKeever, 2011).

Shallow traps are unstable as low energies are required to empty them. To eliminate this unstable part of the signal, in both TL and OSL, a preheat or pause may be applied in the readout protocol before readout. In other cases, residual signals may also interfere with the signal of interest. The residual signal may originate from natural background exposure or previous experimental exposures. It can be depleted thermally by annealing methods (TL/OSL materials) or through optical means (OSL materials), i.e. bleaching (Waldner et al, 2020).

Annealing is also used before reuse of TL materials to empty traps. Most commercial dosemeters are reusable. However, this is only true if the detector materials do not experience any sensitivity changes. An increase or decrease in signal yield means the sample has been de-/sensitized (Bos, 2001; Poston, 2003; Kortov, 2007). Thus, previous calibrations will no longer be valid.

In correspondence with sensitivity changes, the signal stability over time may also change. This can be investigated by studying how the signal changes after a certain time has passed since exposure. Fading is referred to as the decay of signal intensity with time. However, in rare cases, the signal intensity can also increase with time, which can be referred to as inverse fading. This phenomena has mostly been observed in OSL and can possibly be corrected for by applying a mathematical correction factor (Bos, 2001; Waldner and Bernhardsson, 2018; Waldner et al, 2020).

To estimate the signal yield per unit absorbed dose and unit weight, a measure referred to a specific luminescence, $c_{spec}$ (counts $Gy^{-1}$ $mg^{-1}$) is used. It is used to calculate the minimum detectable dose (MDD), which is defined according to equation 1.

$$MDD = \frac{3 \cdot SD}{c_{spec}}, \quad (1)$$

where SD is the standard deviation of the background signal from un-irradiated dosemeters. The MDD is based on 1 SD. Apart from MDD, the specific luminescence can also indicate whether a material has a high or low radiation sensitivity, the specific luminescence should be high and the background signal low. The minimum measurable dose (MMD) is another measure, used to estimate whether the signal is quantifiable (Currie, 1968; Christiansson, 2014).

To observe how the signal changes after the stimulation of traps, TL/OSL-signal curves are observed (Figure 1). TL-signal curves are referred to as glow curves, since the depletion of the signal is shown as a function of the temperature. TL-materials often exhibit two peaks or more, depending on which material is used, and e.g. heating rate. The peaks in a glow curve represent the luminescence from emptied traps at specific energies, corresponding to certain temperatures (Bos, 2001; Poston, 2003). During OSL stimulation, the entrapped signal is released and exponentially depleted (Bøtter-Jensen, 2000; Thomsen, 2004; Yukihara and Mckeever, 2011).

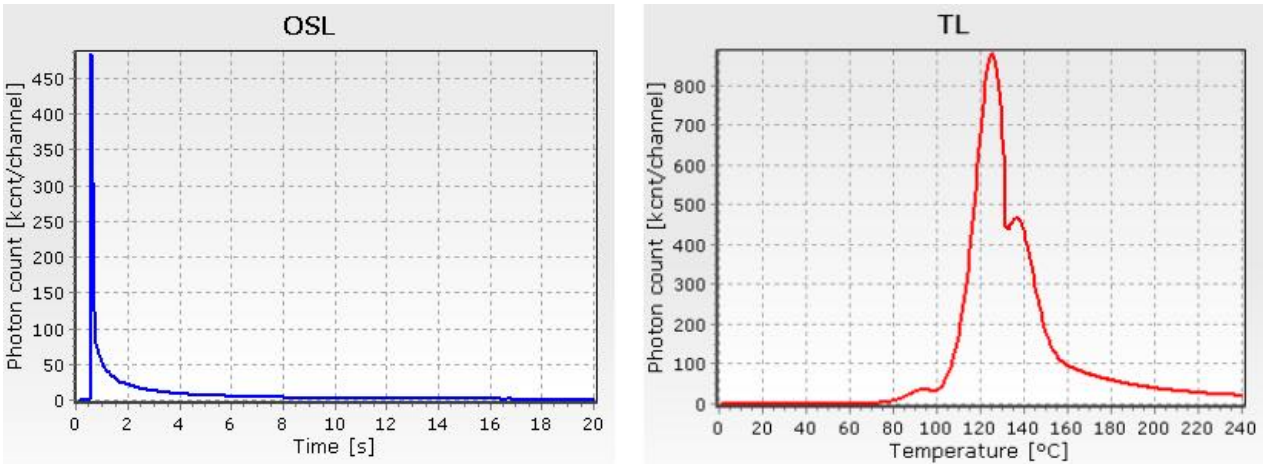


**Figure 1:** OSL signal curve (NaCl) and TL glow curve (LiF) for 60.7 GBq of $^{99m}$Tc.

## 2.4 Clinical application in nuclear medicine at SUS Malmö

Personal dosimetry is implemented in workplaces that require momentary or constant monitoring of personnel, to determine the amount of absorbed dose they receive. The radiation exposure to the staff members of NM departments is monitored by monthly readout of personal TL- or OSL dosemeters. An electronic personal dosemeter (EPD), can also be worn during special occasions, as a complement or cautionary tool. The EPD gives a direct readout and may have an alarm for high dose rates (Sylvain and Bernard, 2002). It can also be compared to the mandatory TLD or OSLD.

The staff members of the nuclear medicine department at SUS Malmö are assigned various tasks involving the radiopharmaceutical and the patient. A radiopharmaceutical is a radioactive pharmaceutical composed of a radioisotope and a carrier. The radionuclides, specifically $^{99m}$Tc, are eluted by one selected staff member in the morning, while another takes care of the preparation of radiopharmaceuticals which will be used during the day. Before each examination, one staff member prepares the radiopharmaceutical that another staff member later will inject into the patient. The same staff members are in charge of taking care of the patient during and after examination, as well as the radioactive waste/leftover in the syringe and injection needle.

For radiation protection, the NM personnel are required to wear a lead apron during the preparation and handling of radiopharmaceuticals before and after patient injection. Personnel are also encouraged to use distance and shielding tools during the preparation and handling of radiopharmaceuticals, since especially their fingers, may be exposed to high radiation doses. In other cases, during the preparation and elution of radiopharmaceuticals at SUS Malmö, the personnel do not have to wear a lead apron, since the time spent in the lab is short and the radiation doses thereby low (Sharp et al, 2005; Bailey et al, 2015).

**Figure 2:** The $^{99m}$Tc elution is prepared with the $^{99}$Mo-generator (left image) and the activity is measured with the ion chamber (right image, Bailey et al, 2015).

## 2.5 Radiation protection

To ensure the safety of the general public or personnel involved in occupational exposure, dose limits were established by the Swedish Parliament (Sveriges Riksdag, SFS 2018:506). According to the Swedish Radiation Safety Authority (SSM) regulation (SSMFS 2018:1), staff members involved in radiation practices are classified into two radiation groups, based on the expected annual effective dose they receive. However, some staff members which are expected to receive a yearly effective dose below 1 mSv may remain unclassified. Category A personnel are expected to receive a higher yearly effective dose than category B. Category A personnel are required to wear a dosemeter and document their monthly personal dose equivalent $H_p(10)$, whereas category B personnel are free to choose whether or not they want to wear a dosemeter.

# 3. Materials and method

## 3.1 Instrumentation

Two versions of the Risø TL/OSL reader (DTU Nutech, Denmark) were used during readout of all three detector materials. The main difference between the readers is the activity and dose rate of the internal $^{90}Sr/^{90}Y$ sources. The older version, DA-15, has a $^{90}Sr/^{90}Y$ beta radiation source of 20 MBq (April 2009), with a current dose rate of 0.6 mGy $s^{-1}$ to NaCl. The newer version, DA-20, has a $^{90}Sr/^{90}Y$ beta radiation source of 100 MBq (October 2019), with a current dose rate of 4.9 mGy $s^{-1}$ to NaCl.

The readers consist of a light stimulation system with blue, green and infrared (IR) LED lamps, a heating system and a photomultiplier tube (PMT). The LED lamps and heater are used to extract the stored information in the trap centers and the PMT is used to detect luminescence. Inside the reader is a sample carrousel, that can hold 48 metal cups for samples during one read. One difference between the two readers is the size of the PMT (different models), meaning there is a difference in efficiency. Another difference between the readers is that DA-20 has an automatic detection and stimulation head (DASH), meaning that the detection filters can be automatically switched (DTU Nutech, 2017).

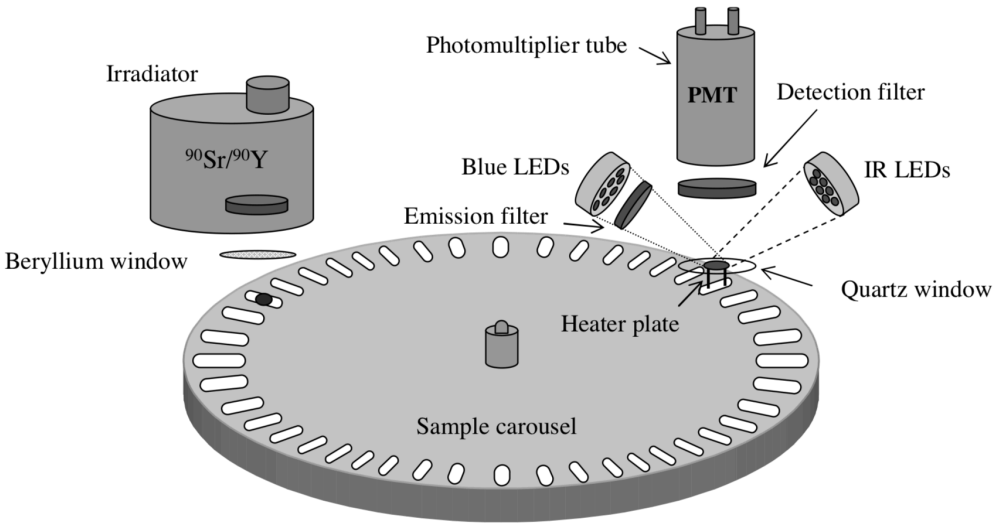


**Figure 3:** A schematic overview of the Risø TL/OSL reader and its components (Thomsen, 2004).

## 3.2 Manufacturing and packaging of detector materials

The TL material used in this study was LiF:Mg,Cu,P, also referred to as MCP-N (Mikrolab, Poland), manufactured in the form of chips with a thickness of 0.9 mm and dimensions of 3.2×3.2 $mm^2$. In order to keep track of which LiF chip was used, the chips were labeled with individual numbers.

However, to avoid attenuation of the luminescence during readout, the labeled side of the chips were facing down on the metal cups of the carrousel in the Risø TL/OSL reader.

$Al_2O_3$, read by OSL, came in the form of discs that had been removed from discarded InLight dosemeters manufactured by Landauer. The $Al_2O_3$ discs have a diameter of 0.7 mm and a thickness of approximately 0.1-0.2 mm. It also consists of a mixture of pulverized crystals and polyester binder, glazed onto a film of polystyrene and enveloped between two polyester foils (Landauer, 2000).

Throughout the study, two different brands of salt, ”Finkornigt salt med jod” (ICA AB, Solna, Sweden), and ”Finkornigt salt med jod” (Falksalt, Salinity AB, Falkenberg, Sweden), were used as OSL detector materials. The salt, with an optimal grain size of 100-250 µm, was pressed into rigid pellets, with a 4 mm diameter and 0.8 mm thickness. A compression force of 0.5 ton was used with a semi-automatic desktop tablet press (TDP 0 Desktop Tablet Press, LFA Machines Oxford Ltd), to produce the NaCl pellets. This was done to improve the homogeneity and response from the salt (Waldner and Bernhardsson, 2018).

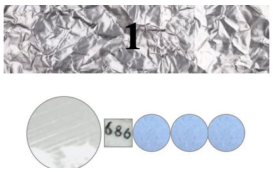


**Figure 4:** Dosemeter kit in row geometry for 1 $Al_2O_3$, 1 LiF and 3 NaCl pellets.

Two geometries for the dosemeter kits were investigated. During the first experiments, a *row geometry* was tested (Figure 4), where 1 $Al_2O_3$ disc, 1 LiF chip and 3 NaCl pellets were placed next to each other in a row.

To reduce the uncertainties from the positioning of the different detector materials, a *stack geometry* was also tested, where all three detector materials were stacked on top of each other: 3 NaCl pellets with 1-3 LiF chip on top, were sandwiched between 2 $Al_2O_3$ discs, according to Figure 5. To ensure no change in moisture levels in the NaCl pellets and to protect the OSL materials from optical bleaching, the materials were enveloped in plastic foil and either four layers of aluminum foil (40 µm thick) or one layer of aluminum tape (100 µm thick).

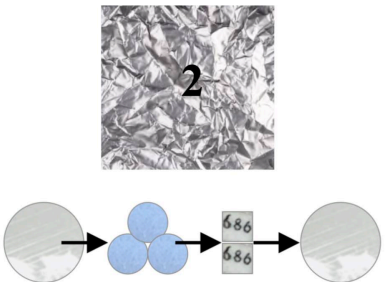


**Figure 5:** Dosemeter kit in stack geometry for 1 $Al_2O_3$, 3 NaCl, 1-3 LiF and 1 $Al_2O_3$.

## 3.3 Calibration and readout

### 3.3.1 Irradiation geometries

Two different irradiation geometries were used for calibration of the TL/OSL detector materials: the internal $^{90}Sr/^{90}Y$ source in the Risø TL/OSL reader at SUS Malmö and the $^{60}Co$ calibration unit at SUS Lund. The aim was to compare the signal to dose responses of all three detector materials for two different irradiation geometries.

**Table 1:** Readout protocol for OSL with NaCl and $Al_2O_3$, as well as TL with LiF.

| | OSL | | TL |
|---|---|---|---|
| **Step** | **NaCl** | **$Al_2O_3$** | **LiF** |
| 1. | **Administration of $D_u$** | | Annealing 240 °C, pre-irradiation, 10 min |
| 2. | Pause during 3600 s | Pause during 100 s | **Administration of $D_u$** |
| 3. | OSL readout, blue LED, 40% optical intensity during 20 s | OSL readout, blue LED, 90% optical intensity during 100 s | Annealing 100 °C, post-irradiation, 10 min |
| 4. | **Administration of $D_c$** | | TL readout, 5 °C/s up to 240 °C, 60 s |
| 5. | Pause during 3600 s | Pause during 100 s | |
| 6. | OSL readout, blue LED, 40% optical intensity during 20 s | OSL readout, blue LED, 90% optical intensity during 100 s | |

At SUS Malmö, signal to dose response curves, as well as other properties of the OSL materials were studied using the internal $^{90}Sr/^{90}Y$ sources in the the Risø TL/OSL readers described in section 3.1. To investigate whether there is a difference in signal to dose response between the older and newer model of the TL/OSL reader, calibrations of NaCl (Falksalt) and $Al_2O_3$ were done with both readers.

The signal to dose response curves were established for an average of 3 $Al_2O_3$ discs, with administered radiation doses ranging up to 300 mGy, in units of dose to $Al_2O_3$. The same was done for NaCl, for an average of 5 NaCl pellets for each dose, in units of dose to NaCl.

The TLDs were calibrated at SUS Lund. A polymethyl methacrylate (PMMA) slab phantom, accommodating 100 samples was positioned in the middle of the radiation field at a specific distance from the $^{60}Co$ source, that was mounted at a 90° degree angle. An ionization chamber was used during the first calibration to measure the dose rate at the defined distance from the source. The dose rate was 4.88 mGy $s^{-1}$ to water, at the position of the PMMA calibration phantom. A total of 99 LiF chips were irradiated six times using this setup with readout and resetting in between. The OSL materials were exposed during one occasion in the $^{60}Co$ beam with the LiF chips, to establish dose response curves for all three materials, administrating radiation doses of 10, 20, 49, 73 and 98 mGy, in units of dose to water ($D_w$). For LiF and $Al_2O_3$, the estimations were done for an average of 3 samples, whereas for the NaCl (ICA) an average of 5 pellets was used for each dose. Using the same setup, fading properties were also investigated. 50 NaCl pellets, 10 $Al_2O_3$ discs and 10 LiF chips were irradiated with a radiation dose of 49 mGy and the signals for 5 NaCl pellets, 1 $Al_2O_3$ disc and 1 LiF chip were read at 10 different occasions from the time of exposure.

### 3.3.2 Readout protocol

Individual readouts of the three materials were done using the TL/OSL readout protocols presented in Table 1. The readout protocol for NaCl pellets has been optimized in earlier works (Waldner, 2017, Waldner and Bernhardsson, 2018). In comparison, the readout protocol for $Al_2O_3$ was compiled after optimizing the readout protocol, e.g. investigating the optimal pause and optical intensity, as well as surveying previous studies.

For $Al_2O_3$, most of the signal can be extracted during the first 20 seconds. The net signal was estimated by integrating over the first 20 (OSL signal) and last 20 seconds (OSL background signal) during stimulation (Geber-Bergstrand, 2017). The same process was repeated for NaCl. In this case, the integration was done over the first 5 and last 5 seconds (Waldner et al, 2020). The OSL-signal curves slightly differ for $Al_2O_3$ and NaCl possibly due to the difference in characteristics, i.e. radiation sensitivity.

The readout protocol for LiF was developed in-house, specifically for the TL/OSL reader but based on manufacturer recommendations (TLD Poland, 2001-2005). Annealing is a requirement for TL-materials before and after irradiation in order to stabilize the traps and prepare the LiF chips for reuse. Before irradiation the LiF chips are annealed in an oven at 240 °C, during 10 minutes and also before TL-readout at 100°C, during 10 minutes (Christiansson et al, 2018). The net signal was integrated over channel 140 and 280.

### 3.3.3 Absorbed dose estimations

Correction factors for residual signals not emptied by the annealing were estimated by calculations based on the numerous calibrations of the LiF chips in the $^{60}Co$ calibration unit. After each calibration, the LiF chips were read and the measured signals were background corrected using 0.14% of the previous signal. The signal per dose for each TLD was calculated and used as correction factors. To estimate the absorbed doses for the LiF chips, equation 2 was used,

$$D_{LiF} = \frac{S_{b,c}}{c_{TLD,LiF}}, \tag{2}$$

where $D_{LiF}$ [Gy] is the estimated absorbed dose, $S_{b,c}$ [counts] is the background-corrected signal after exposure and $c_{TLD,LiF}$ [counts $Gy^{-1}$] is the conversion factor for a specific LiF chip. The absorbed dose estimations for the LiF chips will be used as a reference for the other detector materials.

To estimate the absorbed doses for the $Al_2O_3$ discs, a calibration (signal to dose response) curve was used. The calibration curve provides a factor used for estimating the absorbed doses by calculating the ratio between the background corrected signals and the calibration factor.

The absorbed dose estimations for NaCl pellets were calculated using a simple equation to relate the unknown and calibrated dose- and signal values,

$$\frac{D_{u,OSLD}}{S_{u,OSLD}} = \frac{D_{c,OSLD}}{S_{c,OSLD}}, \quad (3)$$

where $D_{u,OSLD}$ [Gy] is the unknown dose after exposure to ionizing radiation during e.g. clinical work or an unintentional exposure, $S_{u,OSLD}$ [counts] is the corresponding signal acquired from the intensity of the exposure, $S_{c,OSLD}$ [counts] is the calibration signal and $D_{c,OSLD}$ [Gy] is the corresponding calibration dose (Waldner and Bernhardsson, 2018).

The detector materials were calibrated in different units of calibration. For the purpose of comparing the dose estimations between all three detector materials, mass energy-absorption coefficients ($\mu_{en}\ \rho^{-1}$) were used to calculate conversion factors, which were used to compensate for the difference in units of calibration and difference in energy dependence (Hubbell and Seltzer, 2004). The calibration factors also compensate for possible interference from the packaging layers.

## 3.4 Dose comparisons at different dose rates

As an initial test of the three types of dosemeter materials included in this work, a test of the dose estimation ability for different dose rates was evaluated.

Ten styrofoam blocks were positioned in a row at increasing distance from a radiation source. A first block had a hole cut through, all the way down to the center, in which a radioactive source was placed, at a defined position in relation to the other styrofoam blocks (Figure 6). Light sealed dosemeter kits, were taped horizontally on the 10 styrofoam blocks, at the same height as the radiation source.

The first block with the dosemeter kit was placed 30 cm from the source. Due to an initial, fast decrease in the dose rate at close distances to the source, a second block was placed at 45 cm from the radiation source to increase the resolution. Apart from the second block, the distance between each block was 30 cm. The last styrofoam block was placed 2.7 m from the source.

Two different setups were used, one with a $^{137}$Cs source with an activity of 266 MBq (Setup 1) and one with a $^{99m}$Tc source with an activity of 61 GBq (Setup 2). The exposure in Setup 1 lasted for five days. The dosemeter kits were configured in the row geometry mentioned in section 3.2 (Figure 4). In contrast, the exposure in Setup 2 lasted about three days. The dosemeter kits used in this measurement were configured in the stack geometry mentioned in section 3.2 (Figure 5). The ICA brand (NaCl) was used for both measurements. A handheld radiation protection instrument (SRV-2000, RADOS, Finland) was placed at each position for 5 minutes on top of the styrofoam blocks, to measure the dose rate, in units of H*(10), as a reference to the dosemeter kits after each setup.


**Figure 6:** Experimental setup for the dose rate measurement. The radiation source is placed in the center of one styrofoam block, placed at one end of the table and the dosemeter kits were attached to the other 10 blocks at different distances from the radiation source.

## 3.5 Measurement of eye doses to staff working with nuclear medicine

Two plain plastic buckets, used for the disposal of injection needles and syringes are positioned behind a wall of lead. For patients under 70 kg, activities of 400 (± 30-50) MBq $^{99m}$Tc are prepared according to a protocol. After injection, approximately 10% of the activity remains in the syringe, which is immediately disposed of by the staff members. A CIRS ATOM dosimetry phantom (male model) was placed on top of a table in front of the disposal garbage bin (Figure 7). The bottom slices of the phantom were removed to simulate a women of average height (165 cm), since most of the personnel at SUS Malmö are women. Dosemeter kits (stack geometry, section 3.2, NaCl - Falksalt) were positioned at different points on the head of the phantom, as well as a couple of positions distributed over the torso. The disposal hatch opens up in an outward 30° angle at chest height. A cylindrical carton was placed in between the wall and the opened hatch, to make sure it avoids closing during the measurement.

The CIRS ATOM phantom was positioned closely to the garbage disposal, accounting for the fact that the staff members tend to lean in when disposing of the injection needles. Due to this, the eyes are exposed to ionizing radiation in the direct radiation field. To accumulate enough signal, the CIRS ATOM phantom was left standing in front of the garbage disposal for 18.6 hours.

The aim of this study was to determine the surface eye doses, as well as the exposure in other points on the phantom to determine the dose distribution in this situation. Also, to study how accurately the different detector materials estimate the absorbed doses in the clinic and how well they agree with one another.

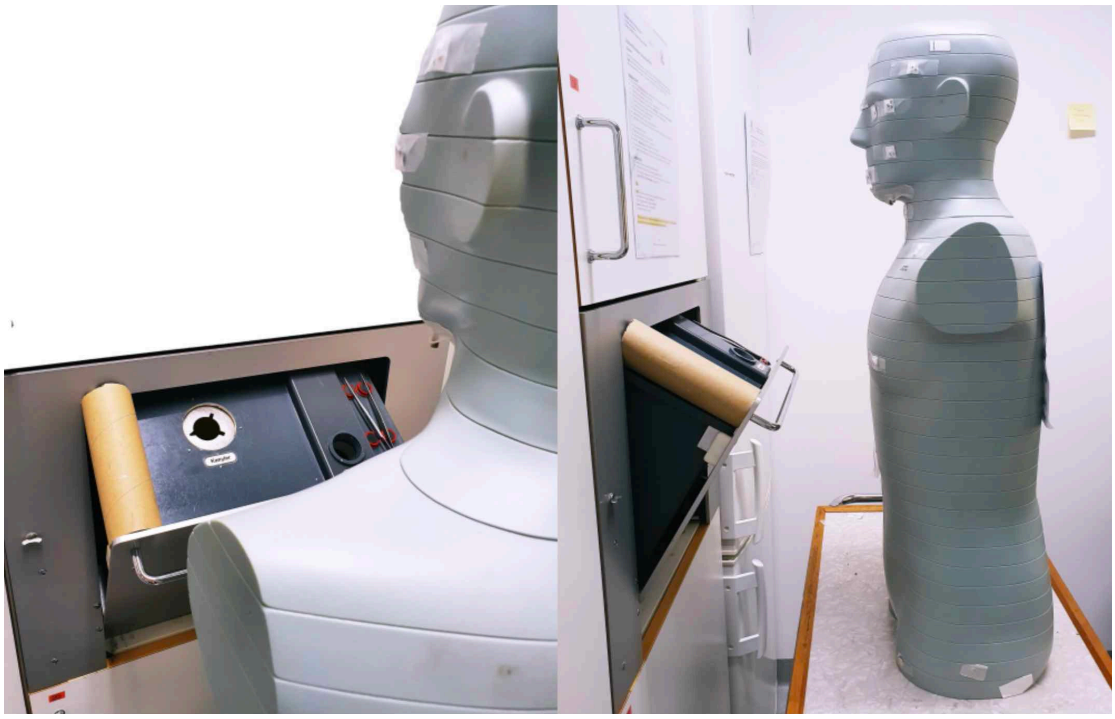

**Figure 7:** Experimental setup for the measurement of absorbed doses to the eyes of hypothetical staff in nuclear medicine, during disposal of radioactive waste using dosemeter kits attached on a CIRS ATOM dosimetry phantom.

## 3.6 Dosimetry with CIRS ATOM dosimetry phantom

A laboratory simulation was established in order to evaluate the absorbed doses to the eyes that NM staff receives when working behind a Laminar Flow Cabinet (LAF) bench, while handling radiopharmaceuticals. It should also be noted that they usually wear a protective lead apron and work behind lead glass while handling the radiation source. However, during this measurement, no shielding was applied. For research purposes, this measurement also shows how well the three dosemeter materials work in relation to each other. It also shows how well different packaging geometries work. With this measurement, it is possible to see what parts of the eyes of the worker that are more or less exposed to the radiation field at the LAF bench.

The CIRS ATOM dosimetry phantom was set up in a laboratory at SUS Malmö according to Figure 8, with protective eyewear taped on the phantom. Dosemeter kits, containing 8×5 NaCl pellets (ICA), were taped on each of the plastic glass of the protective eyewear.

Using the row geometry (section 3.2, Figure 4), three kits were prepared and taped on the frames of the eyewear, one on each side of the frame and one between the eyes. Two additional kits, prepared with the stack geometry (section 3.2, Figure 5), were positioned on each corner of the glasses since commercially available eye lens dosemeters are often attached at the side of the head. However, this geometry only included one pellet of each detector material. The dosemeter kits taped on the protective eyewear would provide an appropriate estimate of the dose distribution at different positions around the eyes, relative to the radiation field. In order to evaluate the surface eye doses, one LiF chip was taped directly on the surface of each eye, and also between the eyes. Additionally, two LiF chips were placed inside dedicated holes in the fifth slice of the phantom, to represent the absorbed eye lens doses.

The radiation source, a glass vial with $^{99m}$Tc with an activity of 60.7 GBq, was positioned 30 cm from the phantom, at waist height. The glass vial was held in position on top of a styrofoam block by a plastic jar. The exposure lasted approximately 2 hours.

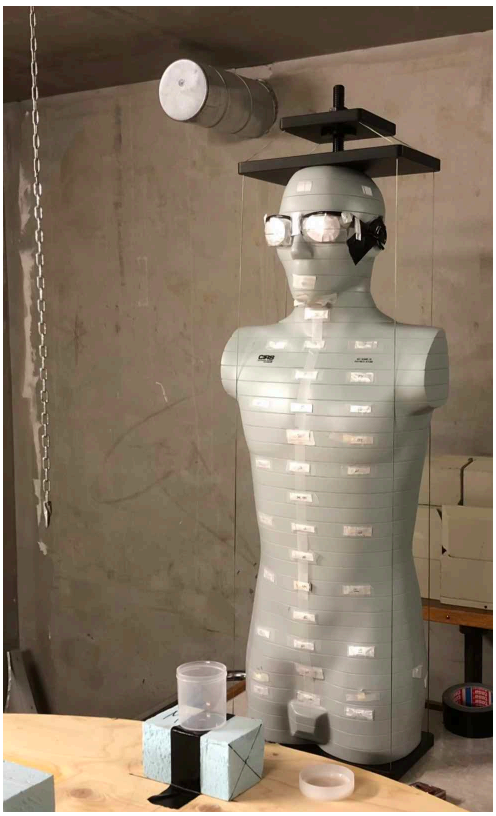

**Figure 8:** Experimental setup for the simulation of staff member working behind LAF-bench with $^{99m}$Tc. Dosemeter kits were attached on the torso and the protective eyewear.

This measurement was repeated with a similar exposure geometry using a $^{137}$Cs point source with an activity of approximately 0.75 GBq, since it has a photon energy similar to $^{18}$F annihilation photons used in Positron Emission Tomography (PET) examinations. The three bottom slices of the phantom, as well as the black stand was removed, to simulate the average height of women, making this measurement more representable to a clinical situation. Since, $^{137}$Cs has a lower activity than $^{99m}$Tc, the measurement lasted 2 days to accumulate enough signal for dose determinations. Dosemeter kits were prepared using the stack geometry (section 3.2, Figure 5, NaCl - Falksalt), and one kit was positioned at each side of the frames and between the plastic glasses, whereas four dosemeter kits were placed on top of the plastic glasses resembling four quadrants.

Additional laboratory simulations were done of situations where a patient has been injected with a radiopharmaceutical. Four different exposure geometries were set up, for different patient groups with different radionuclide uptake. In the first two setups, $^{99m}$Tc pertechnetate was used and in the last two setups, $^{137}$Cs was used to simulate PET examinations using $^{18}$F. The stack geometry (section 3.2, Figure 5) was used for all four measurements. In the last setup, a couple of dosemeter kits using the row geometry (section 3.2, Figure 4) were also added. The ICA brand was used for Setup 1 and 2. Falksalt was used for half the dosemeter kits in Setup 2, as well as for all dosemeter kits in Setup 3 and 4.

This study aims to show how the radiopharmaceuticals distributed in the patient will affect, in terms of radiation field, different parts of a person standing close to the patient. This study proves useful as reference to when staff members and the general public are in close contact to the patient (directly after the radioactivity had been distributed). Furthermore, all three detector materials will be compared in the different positions of the phantom, as well as to one another. This measurement will show how well the regular personal dosemeter, worn at chest height, represents the overall absorbed dose to the body in reference to other positions on the body.

In Setup 1 and 2, free $^{99m}$Tc pertechnetate was used. For such radiopharmaceutical, the activity is distributed over the brain, the thyroid gland, the stomach, kidneys and bladder. However, in Setup 1, the focus was directed on all activity being distributed to the brain. For Setup 2, a situation was simulated where $^{99m}$Tc-tetrofosmin (Myoview), used for heart examinations, was injected in the patient. The activity is mainly distributed to the heart and partially to the bladder.

Two different physical phantoms were used (Figure 9): one dark phantom representing the patient (RANDO, Alderson Research Laboratories, USA) and one light phantom representing a person standing next to the patient (CIRS ATOM dosimetry phantom, male model). Dosemeter kits were placed at defined positions over the torso and head of the CIRS ATOM phantom to measure the obtained absorbed dose from the radiation emitted from the patient.

In Setup 1, the RANDO phantom was prepared by substituting part of the head with two plastic bottles filled with 500 ml water, injected with equal amounts of $^{99m}$Tc (total activity of 2.59 GBq). The dose rate was also measured at a distance of 20 cm from the injected water bottles with a handheld instrument (RAM GENE-1, Rotem, Israel), to verify whether the activity had been equally distributed to the water bottles.

**Figure 9:** Experimental Setup 1 and 2 for the simulation of radiopharmaceutical distribution of $^{99m}$Tc in the brain (left) and torso (right). The light phantom (CIRS ATOM) represents the staff member and the dark phantom (RANDO) represents the injected patient.

In order to measure the absorbed dose a person standing next to the patient would receive, the CIRS ATOM phantom was placed at a distance of 30 cm from the RANDO phantom, at an angle of approximately 45°. The exposure lasted one day.

In Setup 2, two 500 ml water filled bottles, injected with $^{99m}$Tc pertechnetate (total activity of 2.55 GBq), with approximately 80% uptake in the heart and 20% uptake in the bladder, were placed approximately where the heart and bladder are located in the RANDO phantom (Figure 9). Another two water filled bottles were placed on each side of the injected bottles to create a slightly more realistic scatter of the radiation source in the chest and bladder (Figure 9). In this setup, the CIRS ATOM phantom was placed at a slightly longer distance (35 cm) from the RANDO phantom and the exposure time was shorter (5 hours).

The previous measurements were repeated in Setup 3 and 4, using a $^{137}$Cs source. In Setup 3, a $^{137}$Cs source (total activity of approximately 0.75 GBq), was positioned in the middle of the head of the RANDO phantom, between two water filled bottles (Figure 10). In the last exposure geometry (Setup 4), the same $^{137}$Cs source was placed at the position of the heart, between four water filled bottles, by removing 2 slices of the chest area in the RANDO phantom. This measurement lasted 4 days, whereas the previous measurement (Setup 3) lasted 2 days.

**Figure 10:** Experimental Setup 3 and 4 for the simulation of radiopharmaceutical distribution of $^{137}$Cs in the brain (left) and in the torso (right). The light phantom (CIRS ATOM) represents the staff member and the dark phantom (RANDO) represents the injected patient.

During both measurements, the CIRS ATOM was placed at a 45 cm distance from the RANDO phantom (Figure 10). Additionally, an EPD (DMC 3000, Mirion, USA) was attached to the CIRS ATOM phantom, above the left chest, for 19 minutes in both setups using the $^{137}$Cs source. This was done as an additional comparison to the passive detectors.

## 3.7 Difference in absorbed dose with and without lead apron during preparation and elution of radiopharmaceuticals

During the preparation and elution of radiopharmaceuticals, the staff members are required to change into sterile overalls, gloves, hair mask and face mask, as well as sterile slippers (Figure 2), due to the sterile environment in the hot lab.

When quantifying the activity of the radiopharmaceuticals using an ion chamber, the syringes are lowered into a well in a cupboard where there is no lead shielding installed, leaving the staffs lower part of the body exposed to radiation. For studying the radiation exposure during these procedures, dosemeter kits using the stack geometry (sections 3.2, Figure 5) were prepared and placed on different positions on the protective overalls (Figure 11). The ICA brand (NaCl) was used during the preparation of radiopharmaceuticals and the other NaCl brand (Falksalt) was used during the elution of radiopharmaceuticals. Since the main focus was directed to the legs, most dosemeter kits were placed there to measure the exposure from the ion chamber. The leg positions (ranging 1-5), start from the thigh and move down. A couple of dosemeters were also attached to the torso.

To compare the difference in exposure with and without a lead apron (lead equivalence of 0.5 mm), selected staff members wore the dosemeter covered overalls for two consecutive days with a lead apron and for two consecutive days without the lead apron during the preparation of radiopharmaceuticals.

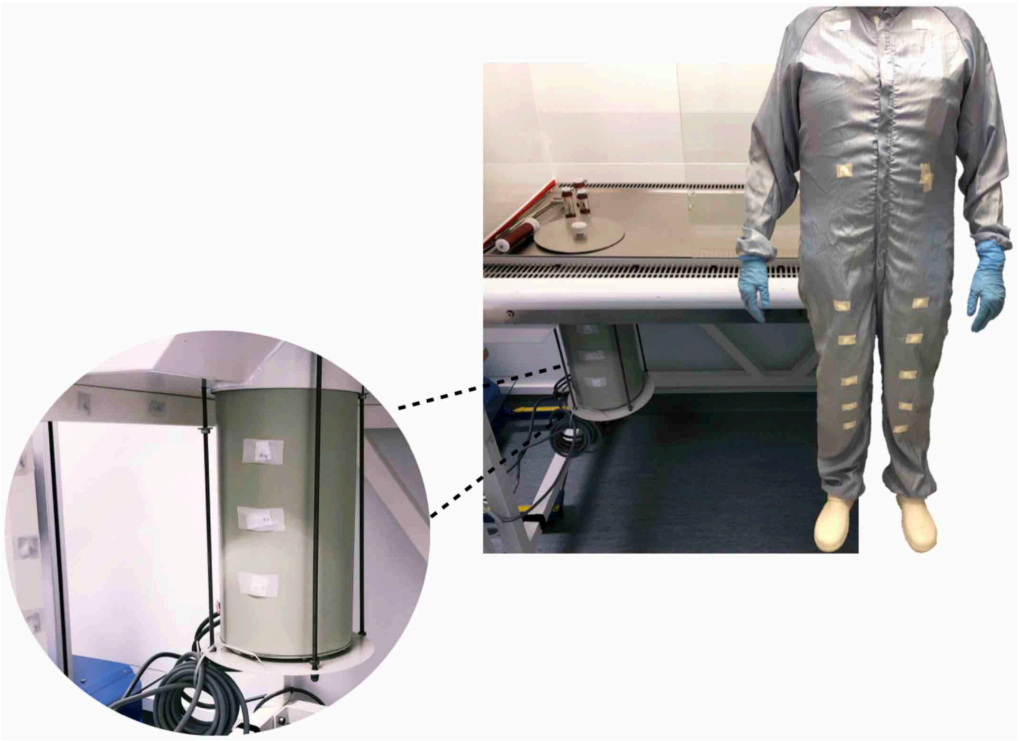

**Figure 11:** The staff member wears a protective overall covered with dosemeter kits in front of an ion chamber during the preparation and elution of radiopharmaceuticals. Dosemeter kits were attached on and around the ion chamber for reference.

The activity and type of radiopharmaceutical were noted during each day, since depending on the examinations scheduled that day, the preparation schedule also changed. A total of 31.4 GBq was prepared during the first two days of the measurement without the lead apron. In contrast, during the other two days a total of 45.4 GBq was prepared (with the lead apron). This measurement was repeated for another staff member during the elution process. It was conducted for one day with a lead apron and another day without a lead apron. A total activity of 83.8 GBq was eluted during the first day (with the lead apron) and a total of 50.6 GBq was eluted during the second day (without the lead apron).

## 3.8 Personal dosimetry for staff members at the nuclear medicine department at SUS Malmö

Dosemeters were prepared with the three detector materials using standard types of LiF dosemeter holders, with the original detector elements removed. These holders are designed to have room for four pellets in a row and were here used with three NaCl (ICA) pellets and one LiF chip. An $Al_2O_3$ pellet was taped onto the holder with plastic tape next to the NaCl pellets. The dosemeter case was enveloped in light-sealing aluminum tape (Figure 12), placed in the plastic badge holder and attached on the staffs' coats at chest height, next to their mandatory dosemeter. The staff usually wears a commercial TLD (Figure 12).

Three of the in-house prepared dosemeters were distributed to the selected NM personnel. The three detector materials, in the in-house prepared dosemeter were compared to the commercial TLD (Figure 12), after one month. One of the staff members for which the dosemeter had been distributed to is classified as category A and only works with $^{18}F$. Since $^{18}F$ has a higher energy and different attenuation properties compared to $^{99m}Tc$, the staff members are more likely to be exposed to higher radiation doses. The other two staff members, that agreed to participate, are categorized as category B and only work with $^{99m}Tc$. This part of the study aims at comparing the monthly dose from the commercial TLD and the in-house made dosemeter.

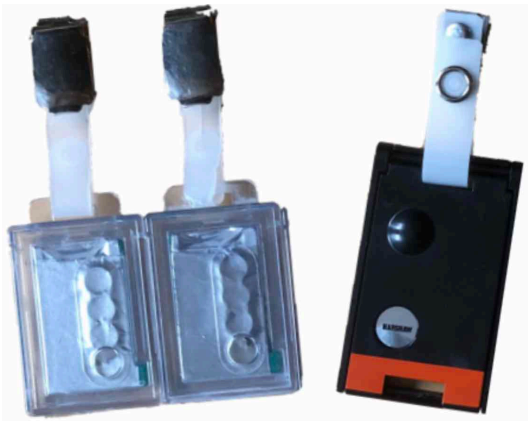

**Figure 12:** Left figure shows self-made dosemeters containing all three detector materials (1 $Al_2O_3$, 1 LiF, 3 NaCl pellets). Right figure shows commercially available TLD worn by medical staff.

# 4. Results and Discussion

## 4.1 Dose response

Figure 13 shows the dose response curves estimated for $Al_2O_3$ and NaCl (Falksalt) in both Risø TL/OSL readers (DA-15 and DA-20, respectively), in units of absorbed dose to salt for NaCl and absorbed dose to $Al_2O_3$ for the $Al_2O_3$ discs.

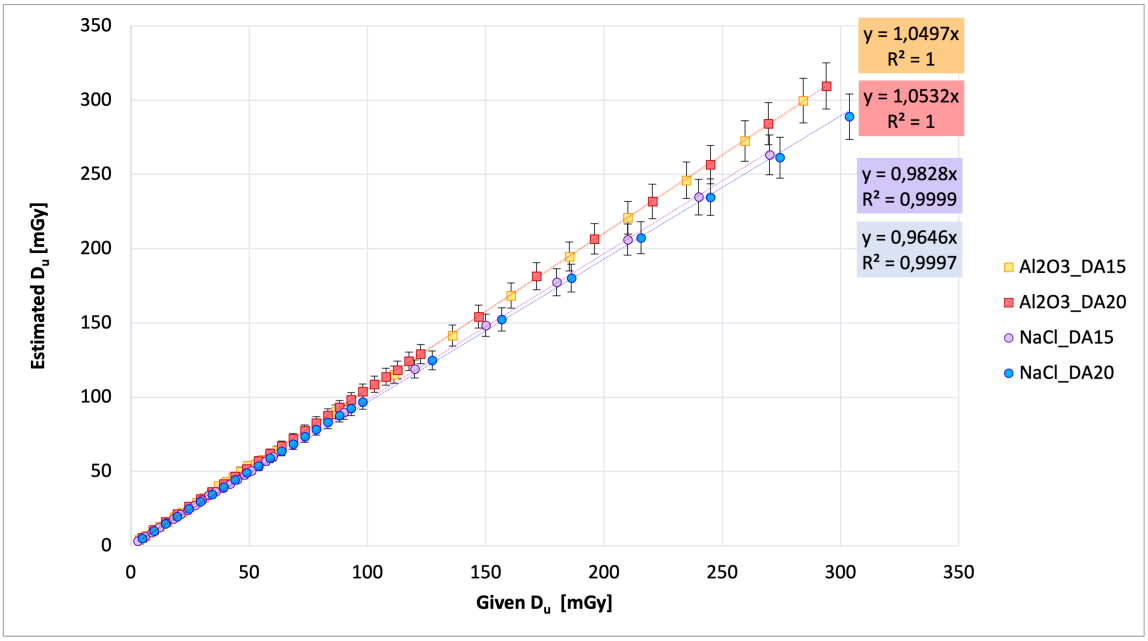


**Figure 13:** Dose response curve for $Al_2O_3$ and NaCl irradiated with the $^{90}Sr/^{90}Y$ source in the Risø TL/OSL reader (DA-15 and DA-20, respectively).

For comparison, the absorbed dose in Figure 13 is referred to as the ”unknown” dose ($D_u$). The given $D_u$ is the administered dose and the estimated $D_u$ is calculated using equation 3. All four dose response curves indicate a linear dose response up to at least 300 mGy. Figure 13 also shows the coefficient of the linear equation for each material and detector, which is approximately 1. Thus, meaning that all four dose response curves are capable of accurately estimating doses. Doses were estimated for an average of three $Al_2O_3$ discs and five NaCl pellets to improve statistics. The uncertainty bars represent 1 standard deviation (SD) of the uncertainty.

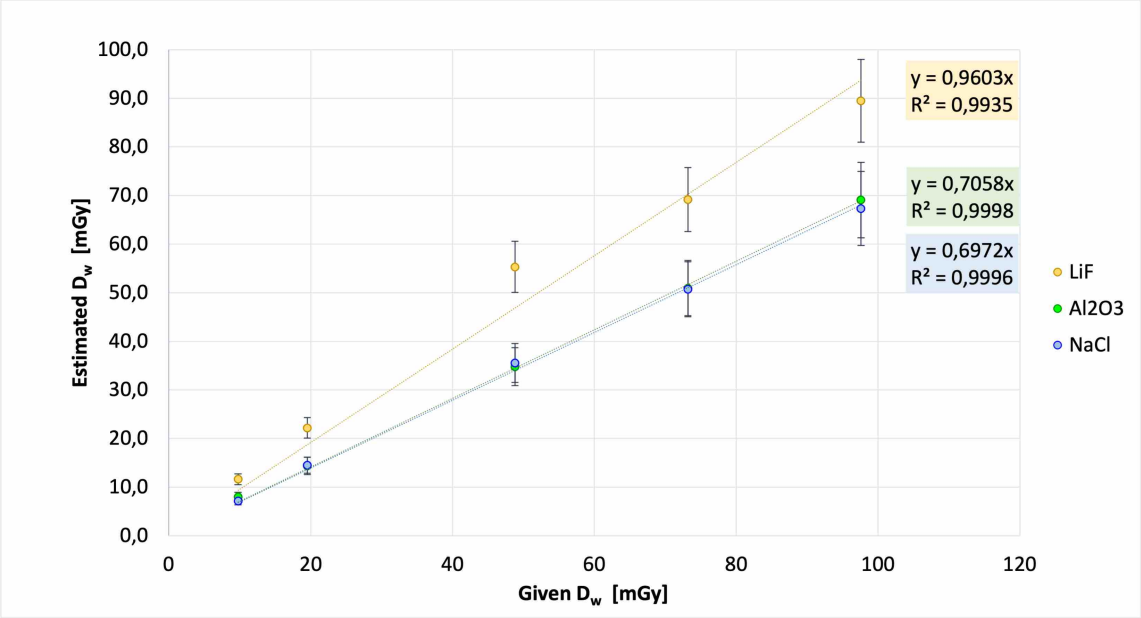


**Figure 14:** Dose response curve for all three detector materials irradiated with a $^{60}Co$ source with a maximum dose rate of 4.88 mGy $s^{-1}$ to water.

After irradiation with a $^{60}Co$ source with a maximum dose rate of 4.88 mGy $s^{-1}$ to water, a large difference is observed between the dose response curves for the TL and OSL materials (Figure 14). After the exposure, it was discovered that one of the monitor lamps inside the room had not been turned off. The monitor lamp was not strong enough to affect the OSLDs during exposure. However, it was in close proximity to the OSL materials during the emptying of the phantom and transfer of the OSL materials into light-tight containers. Since, the OSL materials are highly light sensitive, it is likely that the signals were partially depleted due to the light from the monitor lamp after exposure. The TL material is not affected by optical stimulation. Hence, Figure 14 indicates that LiF has the best dose response. This can also be concluded from the coefficient of the linear equation as it is approximately 1, whereas the coefficient for the OSL materials is approximately 0.7. A potential reason for the inferior dose response, seen for both OSL materials, may be that the administered $D_{c,OSLD}$ during the calibration and readout was too low, which led to an underestimated dose response. In Figure 14, estimations were averaged over three LiF, three $Al_2O_3$ and five NaCl chips and uncertainty bars representing 1 SD were applied. The third data point for LiF falls within 2 SD, due to the relatively high uncertainty.

## 4.2 Fading

50 NaCl (Falksalt) pellets, 10 $Al_2O_3$ discs and 10 LiF chips were administered a total radiation dose of 49 mGy, in units of a $D_w$, from the $^{60}Co$ source. Readouts of the detector materials were done over time. The estimated doses are shown as a function of time after irradiation (Figure 15). The results show an apparent inverse fading of the dose for the NaCl pellets. The estimated dose increases rapidly during the first few hours and slowly days after irradiation. This is a consequence of a decreasing signal yield of the calibration signal over time. In reference to equation 3 (section 3.3.3), a decrease in the calibration signal $S_{c,OSLD}$, will lead to an increase in $D_{u,OSLD}$.

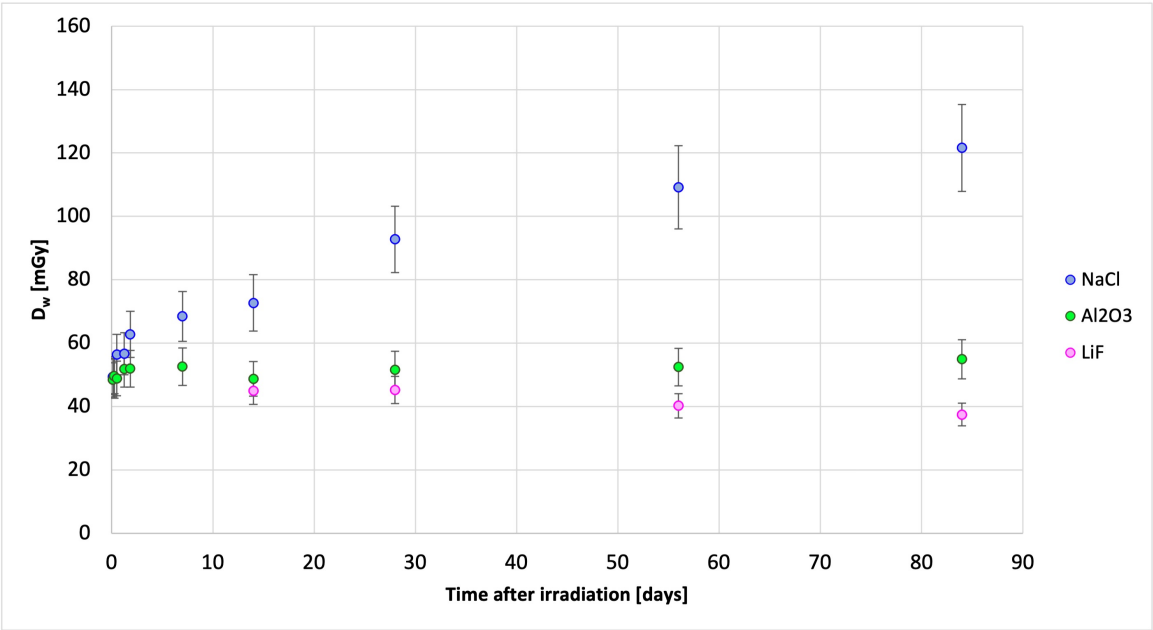


**Figure 15:** Dose estimations as a function of days after irradiation, for all three detector materials after exposure with a $^{60}Co$ source.

In comparison, taking all uncertainties into account, no fading occurs for the $Al_2O_3$ discs, only showing some fluctuations in the dose estimates. In comparison, the LiF chips indicate low fading. The monitor lamp is a source of uncertainty in this measurement as well.

## 4.3 Dose comparisons at different dose rates

In Figure 16, the estimated absorbed dose to air ($D_{air}$) values, normalized to the maximum $D_{air}$ at the first distance from the source, are shown as a function of the defined distances between the dosemeter kits and the $^{137}Cs$ source. The estimated $D_{air}$ values decrease according to the inverse of the squared distance, ($1/r^2$), with increased distance, r. Since the results were normalized against the highest $D_{air}$, all series begin at 1. On average, the results for all three detector materials agree within 35% in relation to one another, up to 1 m from the source. At the closest point to the radiation source, the highest $D_{air}$ values were estimated between 16-31 mGy for all five detectors. The difference in detector response is probably due to the difference in in radiation sensitivity and short distance to the radiation source, which is a consequence of a non-homogenous radiation field. However, as the distance increases, the dose rates decrease and the normalized dose values start to overlap. At the last few points, the radiation field is homogenous over the dosemeter kits and the difference in dose rate is negligible. Hence, the normalized dose values are more agreeable further away from the source. There are some deviations in the estimations for $Al_2O_3$ discs after the first few points, probably as the signals are below the rather high MDD and MMD of the $Al_2O_3$ (1.8 mGy and 5.9 mGy, respectively). Moreover, a NaCl data point at 1.5 m also indicates a higher response, probably due to variations in the measurement or the background signals. However, the reason is not clear.

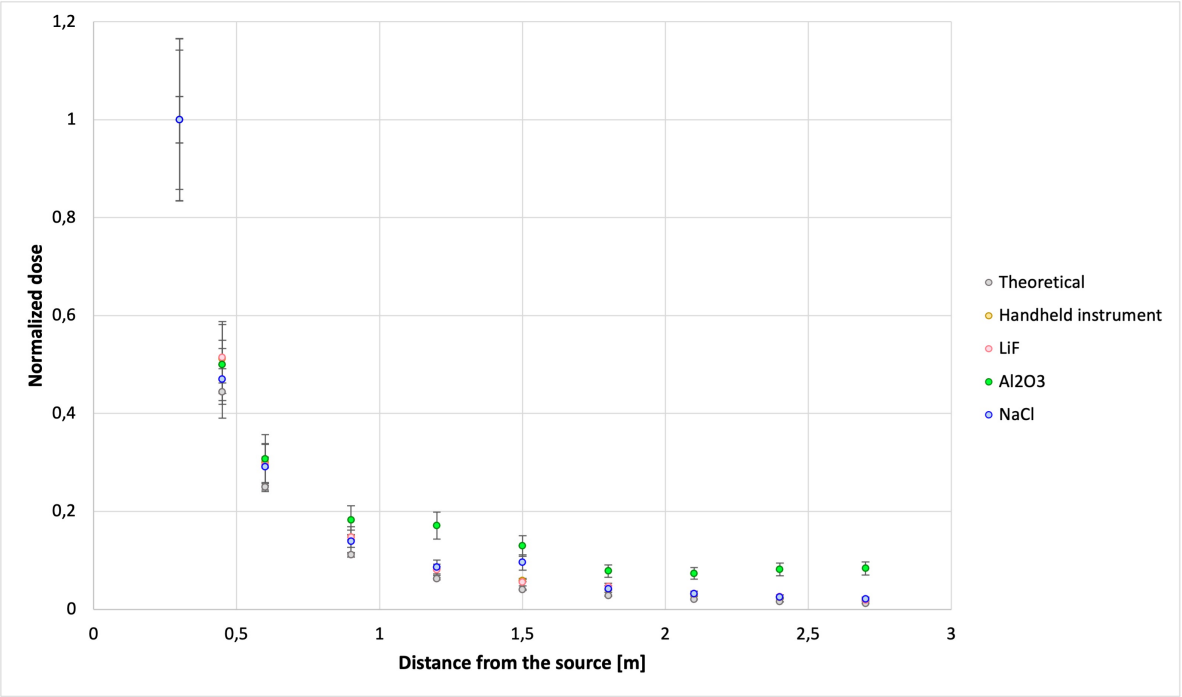


**Figure 16:** $D_{air}$ estimations normalized against the point closest to the radiation source for all five series as a function of distance in relation to the $^{137}Cs$ source.

The detector materials also show good agreement with the handheld instrument and the theoretical calculations, especially at longer distances. A source of uncertainty for the handheld instrument is the sensitivity in its positioning, as it affects the accuracy of the dose rate measurement. As a consequence, the theoretical calculations might also suffer from this as that was based on the dose measured by the handheld instrument at the position closest to the radiation source.

In comparison, the results in Figure 17 for the other irradiation geometry with $^{99m}$Tc display more agreeable results between the three detector materials. The difference between LiF and NaCl for the first few data points is lower compared to the previous measurement. There is an on average 5% difference between LiF and NaCl, whereas the difference in the previous measurement was 35%.

The $D_{air}$ values estimated at the point closest to the radiation source were between 53-58 mGy for all five series. As a result of the higher doses with the $^{99m}$Tc source, higher signals are accumulated which in turn sufficiently suppress the background signals in the $Al_2O_3$ discs. Since, the activity is higher compared to the prior measurement, the dose rates are also higher at different positions in relation to the source.

The detector materials show agreeable results for lower dose rates, probably due to the homogeneity of the radiation field. In comparison to the previous measurements, the handheld instrument shows some deviations for the last few data points. This could be due to the placement of the detector, as it is position sensitive. Also, energy correction factors were used as compensation, due to the difference in energy response. However, this does not affect the normalized estimations.

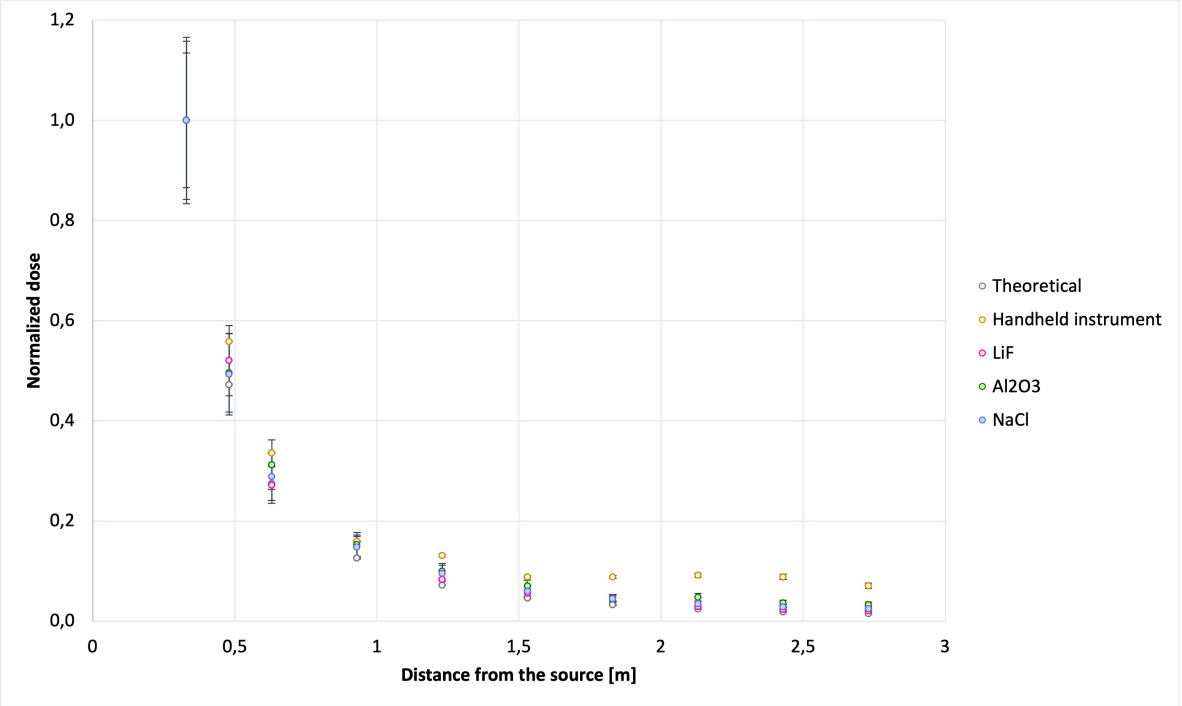


**Figure 17:** $D_{air}$ estimations normalized against the point closest to the radiation source as a function of distance in relation to the $^{99m}$Tc source.

## 4.4 Laboratory simulations with anthropomorphic phantoms

### 4.4.1 Eye doses to NM staff in front of a radioactive disposal bin in the clinic

Figure 18 shows the distribution of the estimated $D_w$ values for LiF and NaCl pellets normalized to the maximum dose rate (30 µSv $h^{-1}$) of the radioactive waste and the total time of the measurement (18.6 h), [Gy $Sv^{-1}$]. Since the daily doses in the clinic are quite low, the signals accumulated by the $Al_2O_3$ discs appeared below detection limits. Hence, they were removed from the results. Longer measurements are required for proper dose estimations using the $Al_2O_3$. It should be noted that this is specific to the discs used in this project and the in-house developed readout protocol.

As indicated in Figure 18, $D_w$ values for LiF and NaCl are in good agreement with each other. The estimations show a difference of up to 30% between LiF and NaCl for the same positions on the phantom. The highest $D_w$ values were estimated around the eyes, at the central positions of the face and on the thyroid, which were positioned in the primary beam of the radiation field from the waste. The lowest $D_w$ values were estimated at each side of the head and on the torso for both LiF and NaCl. The mean uncertainty for all $D_w$ values for the LiF is 19% and for the NaCl pellets it is 28%. Nonetheless, considering the results indicate rather low dose estimations, there is no need for concern regarding the absorbed eye doses to the NM staff during such garbage disposal. Supposing the NM staff members stand in front of the disposal bin for 5 seconds, 10 times a day, the accumulated absorbed dose to the left eye would correspond to 2 µGy/month (using LiF as a reference).

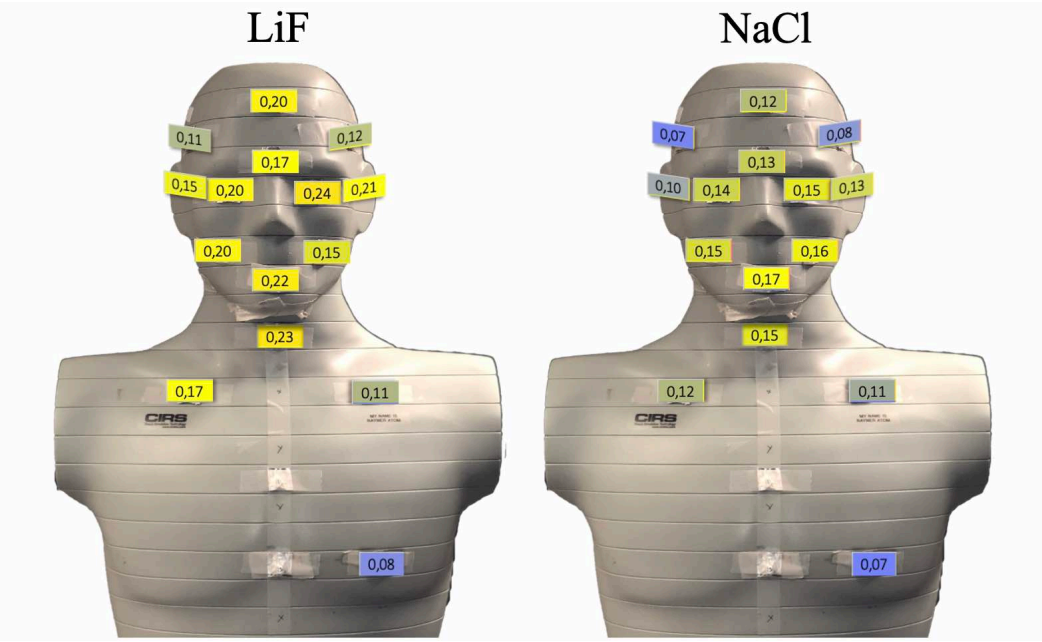


**Figure 18:** Normalized $D_w$ values (ranging from low-blue to high-orange) estimated for LiF and NaCl at 15 different defined points on the CIRS ATOM dosimetry phantom. The estimations were normalized to the maximum dose rate (30 µSv $h^{-1}$) and total time of the measurement (18.6 h), [Gy $Sv^{-1}$].

### 4.4.2 Eye doses in front of a LAF-bench with radiopharmaceuticals

Figure 19 shows the estimation of the surface doses to the eyes (on protective eyewear) in units of $D_w$, normalized to the total activity of the $^{99m}Tc$ source (60.7 GBq at the beginning of the measurement, t = 0) and the total time of the measurement (2.2 h), [µGy GBq$^{-1}$ h$^{-1}$]. As a first approximation, the activity was considered to be the same during the exposure. This is true for all measurements concerning $^{99m}Tc$. Normalized $D_w$ values for each individual NaCl pellet in the 5×8 ordered grid geometry over each eye were estimated, as well as the NaCl pellets positioned at each side of the frames, the corners and between the glasses. The bottom rows have on average higher normalized dose values (18-22 µGy GBq$^{-1}$ h$^{-1}$) as compared to the rest of the positions on and around the eyewear. The cause for this is probably the shorter distance to the radiation source, as compared to the upper rows of NaCl pellets on the glasses. Assuming the true absorbed dose for the NaCl is around the center of the eyes (18-22 µGy GBq$^{-1}$ h$^{-1}$), NaCl pellets placed at the corners and between the eyes show less accurate dose estimations compared to the sides of the frames or directly on the surface of the glasses.

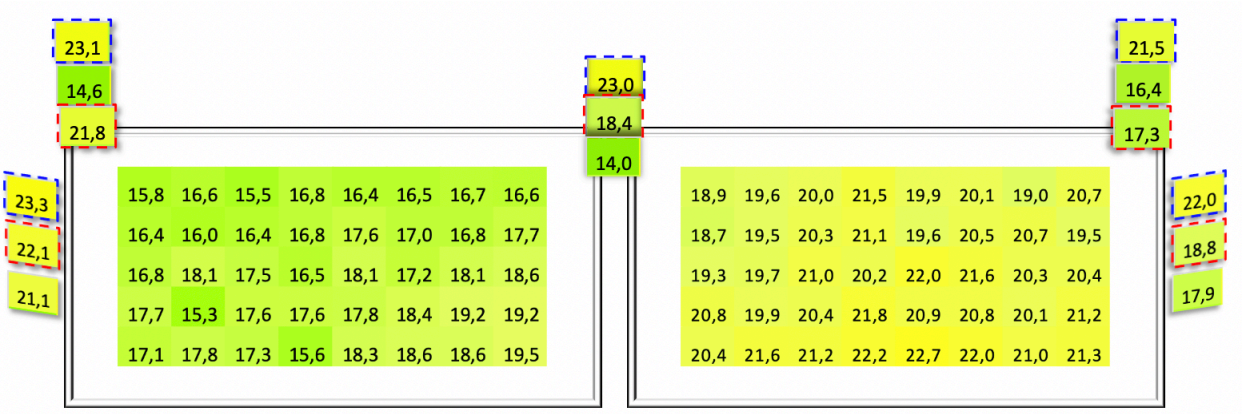


**Figure 19:** $D_w$ values (ranging from low-blue to intermediate-yellow) normalized to the total activity (60.7 GBq at t = 0) and time (2,2 h), [µGy GBq$^{-1}$ h$^{-1}$], of the $^{99m}Tc$ source for the right (left frame) and left (right frame) eye lens for 5×8 NaCl pellets, for LiF (red contoured squares) and $Al_2O_3$ (blue contoured squares) placed at the corner and sides of the frames, as well as between them.

The red contoured squares in Figure 19 show the normalized $D_w$ values for the LiF chips at different positions on the frames. Likewise, the blue contoured squares indicate normalized $D_w$ values for the $Al_2O_3$ discs. The normalized dose values for each detector material are shown in Figure 19 according to their position in the dosemeter kit. The two LiF chips that were placed inside the eyes of the phantom estimated a normalized $D_w$ value of 19.5 and 19.9 µGy GBq$^{-1}$ h$^{-1}$, respectively in the left and right eye. The normalized $D_w$ values of the LiF chips on the surface of the eyes were 25.0 and 20.4 µGy GBq$^{-1}$ h$^{-1}$, respectively for the left and right eye. Based on the absolute dose values, there was a 22% difference between the surface and inside estimations of the left eye and a 3% variation between surface and inside estimations of the right eye. Between the eyes, the normalized $D_w$ value was estimated at 18.4 µGy GBq$^{-1}$ h$^{-1}$.

One source of uncertainty, regarding the difference in dose estimations, was the position of dosemeter kits on the protective eyewear. The dosemeter kits were not aligned with one another. Thus, some dosemeter kits were at a slightly longer distance from the radiation source, compared to other positions. This is also true for the positions of the detector materials inside the dosemeter kits, specifically for the row geometry. LiF and NaCl pellets are in better agreement than $Al_2O_3$ and NaCl. For $Al_2O_3$, the $D_w$ values were estimated near 2 mGy, which is also close to the MDD for the $Al_2O_3$ discs. The uncertainties in $D_w$ estimations at each side of the frames and between the frames is probably due to the uncertainty in position since the row geometry was used. The mean uncertainty for all $D_w$ values for LiF is 12%, for the $Al_2O_3$ it is 13% and for NaCl pellets it is 14%.

Figure 20 shows the distribution of $D_w$ normalized to the total activity of $^{137}Cs$ source (~0.75 GBq) and total time of the measurement (96 h), [mGy GBq$^{-1}$ h$^{-1}$], for all three detector materials. All three detector materials show reasonably good agreement in the dose estimations (10-17 mGy) in relation to the irradiation source for this exposure geometry and doses. However, LiF and $Al_2O_3$ seem to be in better agreement with one another.

The lowest normalized $D_w$ values were estimated between 0.12-0.15 mGy GBq$^{-1}$ h$^{-1}$, at each side of the frames of the glasses. The highest $D_w$ values were estimated at different positions on the centre of the glasses. LiF estimated the highest $D_w$ value at the left eye, the third quadrant at 0.24 mGy GBq$^{-1}$ h$^{-1}$. This corresponds to an absolute dose value of 17.2 mGy. The reason for this deviating estimate is unclear. However, this particular LiF chip could have been damaged, thereby estimating the wrong $D_w$ due to inaccurate calibration. The mean uncertainty for all absolute $D_w$ values for LiF is 15% and for the $Al_2O_3$ and NaCl pellets it is 17%.

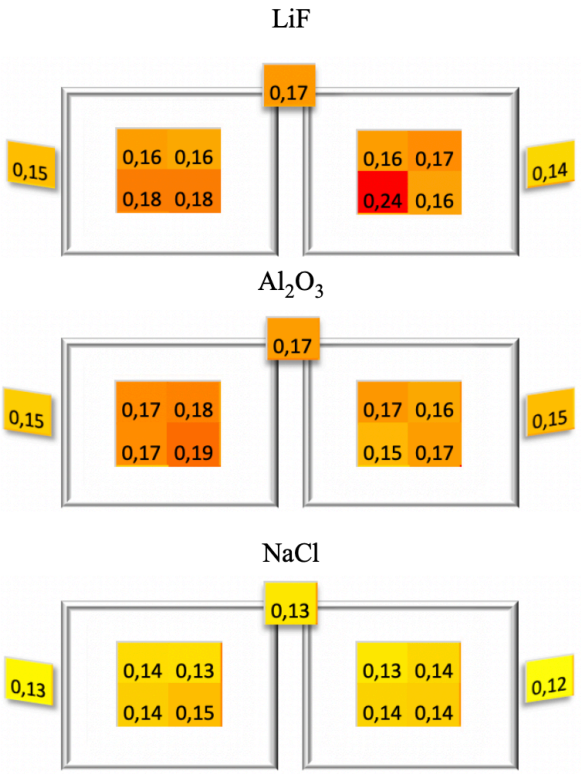


**Figure 20:** $D_w$ values (ranging from intermediate-yellow to high-red) normalized to the total activity of the $^{137}Cs$ source (~0.75 GBq) and total time of the measurement (96 h), [mGy GBq$^{-1}$ h$^{-1}$], to the right (left image) and left (left image) eye for all three detector materials.

NM staff members work relatively fast when preparing the radiopharmaceuticals. Since they are shielded from the main radiation exposure while standing behind lead glass, the absorbed doses to the eyes are relatively low. Using these two measurements as a reference, the actual doses would be considerably lower if the phantom had been shielded with lead in front of the radiopharmaceutical.

### 4.4.3 Radiation exposure of staff from patients after injection of radiopharmaceuticals

Figure 21 shows normalized $D_w$ values for the radiation exposure in a simulation of a NM staff member during the handling of a patient that had been injected with $^{99m}$Tc-pertechnetate and where all activity had been distributed to the head.

The estimations are normalized to the total activity of the $^{99m}$Tc source (2.59 GBq at t = 0) and total time of the measurement (25.7 h), [µGy GBq$^{-1}$ h$^{-1}$]. As indicated by Figure 21, the highest $D_w$ values are observed on the surface of the head and mainly on the left side, due to the positioning of the phantoms in relation to each other. Since the two phantoms are of equal height, the upper parts of the CIRS ATOM phantom, mainly the head, received the highest $D_w$ values. This is observed by all three detector materials (Figure 21). Consequently, the lowest $D_w$ values were measured at the lower parts of the phantom. However, for the $Al_2O_3$ discs, the dose values around the torso appeared below MDD. Thus, they were removed from this measurement.

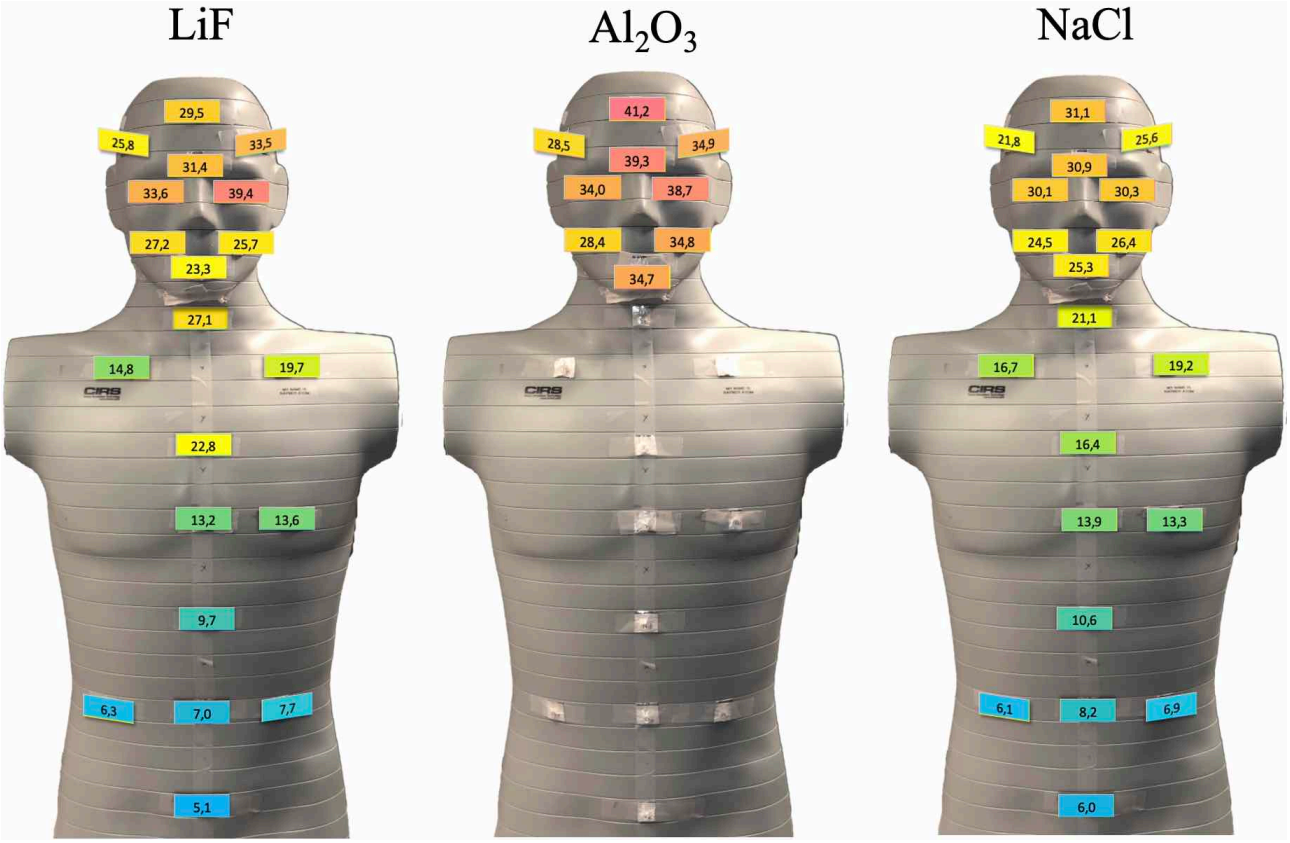


**Figure 21:** Estimated $D_w$ values (ranging from low-blue to high-red) for LiF, $Al_2O_3$ and NaCl, normalized to the total activity of the $^{99m}$Tc source (2.59 GBq at t=0) and total exposure time (25.7 h), [µGy GBq$^{-1}$ h$^{-1}$], for the laboratory measurement with activity uptake in the head. The color scale ranges from lowest (blue) to highest (red) estimated $D_w$ values.

The results further show that the distribution of the $D_w$ values for LiF and NaCl are similar. The mean uncertainty for all $D_w$ values for the LiF is 11 %, for $Al_2O_3$ it is 5% and for the NaCl pellets it is 12%.

It can also be noted that the position where the regular personal dosemeter usually is located, does not provide a representable overall dose estimation in this exposure geometry. The overall representable dose, indicated by the breast dosemeter, provides a basis for calculating the effective dose. Since majority of the sensitive organs are located around the torso, a higher absorbed dose to the head will not contribute much to the effective dose.

The estimated $D_w$ values normalized to the total activity of the $^{99m}$Tc source (2.54 GBq at t = 0) and total time of the measurement (5.05 h), [µGy GBq$^{-1}$ h$^{-1}$], for a similar situation using $^{99m}$Tc-pertechnetate, distributed to the chest and bladder, are shown in Figure 22 for LiF and NaCl. In comparison to Figure 21, these values indicate that the dosemeter kits placed around the head accumulated the lowest absorbed doses. In turn, the lower parts of the body, which were in the center of the two radiation fields (one from the chest and one from the bladder area), accumulated the highest $D_w$ values. The normalized estimations shown in Figure 22 indicate that NaCl shows higher dose estimations in comparison to the LiF chips. In regards to the absolute dose values, the estimations differ up to 35% between NaCl-LiF. The mean uncertainty for all $D_w$ values for the LiF is 11% and for NaCl it is 15%.

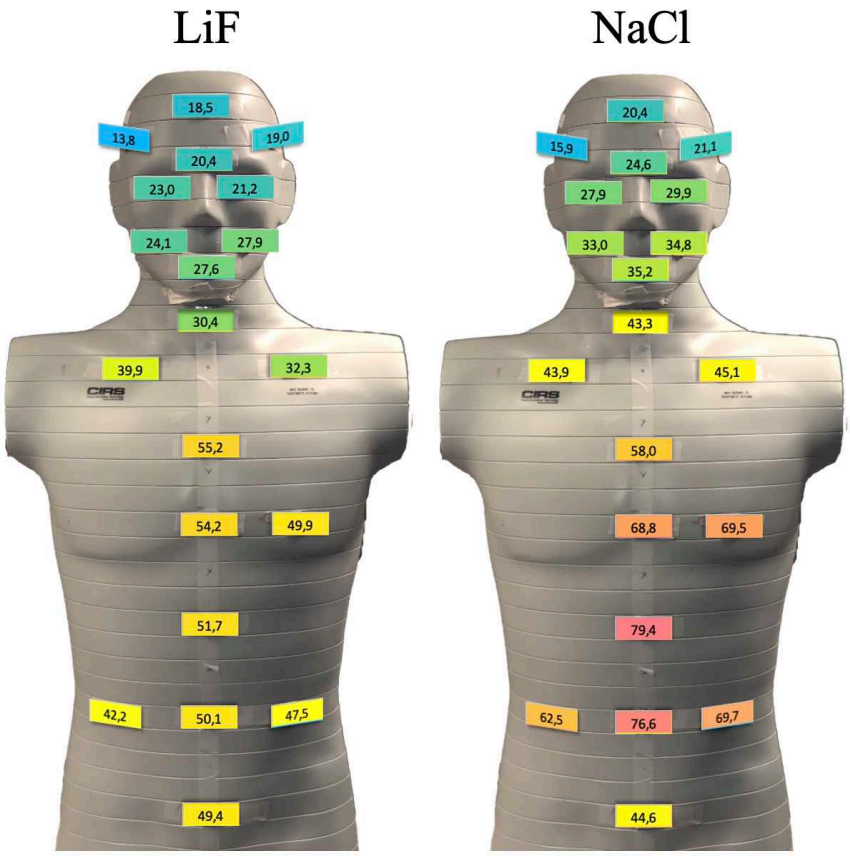


**Figure 22:** Estimated $D_w$ values (ranging from low-blue to high-red) for LiF and NaCl, normalized to the total activity of the $^{99m}$Tc source (2.54 GBq at t=0) and total exposure time (5.05 h), [µGy GBq$^{-1}$ h$^{-1}$], for the laboratory measurement with activity uptake in the torso. The color scale ranges from lowest (blue) to highest (red) estimated $D_w$ values.

The reason for the difference in detector response between LiF and NaCl is currently unclear. The LiF chips had been repeatedly used for a couple of months. One potential explanation could be that the LiF chips have to be re-calibrated after one to two months of usage. Another potential explanation could be the difference in time between irradiation and readout. Extending the pause time could lead to a decrease in efficiency, which would affect the detector response.

The next two figures 23-24 show results for a similar exposure setup using a $^{137}Cs$ point source positioned in the head of the phantom. Distributions of the normalized $D_w$ values for the measurement in which all activity had been distributed to the head are shown in Figure 23. The $D_w$ values were normalized to the total activity of the $^{137}Cs$ radiation source (~0.75 GBq, t = 0) and the total exposure time (50 h), [µGy $GBq^{-1}$ $h^{-1}$].

Both OSL materials show lower dose estimations in reference to the LiF chips – opposite to the $^{99m}Tc$ exposure (Figure 23). As mentioned in the previous measurement, the LiF chips may require additional calibration. Another source of error, throughout the assessments, is related to the $Al_2O_3$ discs and the readout protocol, which was temporarily developed in-house. Furthermore, the administered calibration dose to the NaCl pellets is based on the dose estimations for the LiF chips, assuming they represent the most accurate dose values. The mean uncertainty for all $D_w$ values for the LiF is 15%, for the $Al_2O_3$ it is 12% and for the NaCl pellets it is 17%.

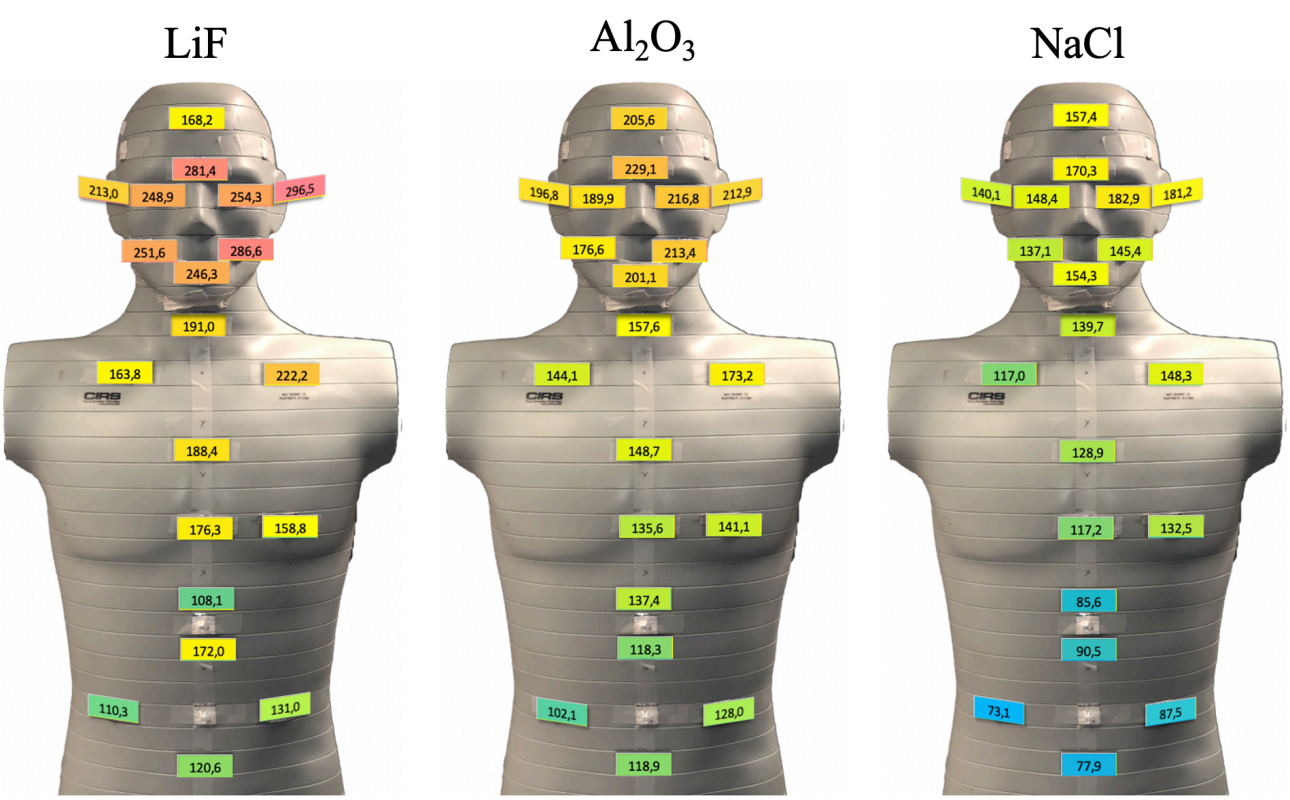


**Figure 23:** Estimated $D_w$ values (ranging from low-blue to high-red) for LiF, $Al_2O_3$ and NaCl, normalized to the total activity of the $^{137}Cs$ source (~0.75 GBq, t = 0) and total exposure time (50 h), [µGy $GBq^{-1}$ $h^{-1}$], for the laboratory measurement with activity uptake in the head.

The EPD at chest height, normalized to the total activity (~0.75 GBq) and exposure time (19 minutes), was 295 µSv $GBq^{-1}$ $h^{-1}$. The corresponding NaCl dose value estimated at chest height was determined as 177.7 µSv $GBq^{-1}$ $h^{-1}$, in terms of personal dose equivalent, $H_P(10)$. There is a 40% difference in the normalized $H_P(10)$, as measured with EPD and NaCl for this exposure geometry. A large part of this discrepancy is related to the positioning of the both detectors on the phantom and exposure time of the EPD.

The other measurement with the $^{137}Cs$ source, when the activity (~0.75 GBq) was distributed to the heart area, shows that all three materials are in better agreement with each other (Figure 24),. Although, the $Al_2O_3$ discs show less deviation in relation to the LiF chips in comparison to the NaCl pellets.

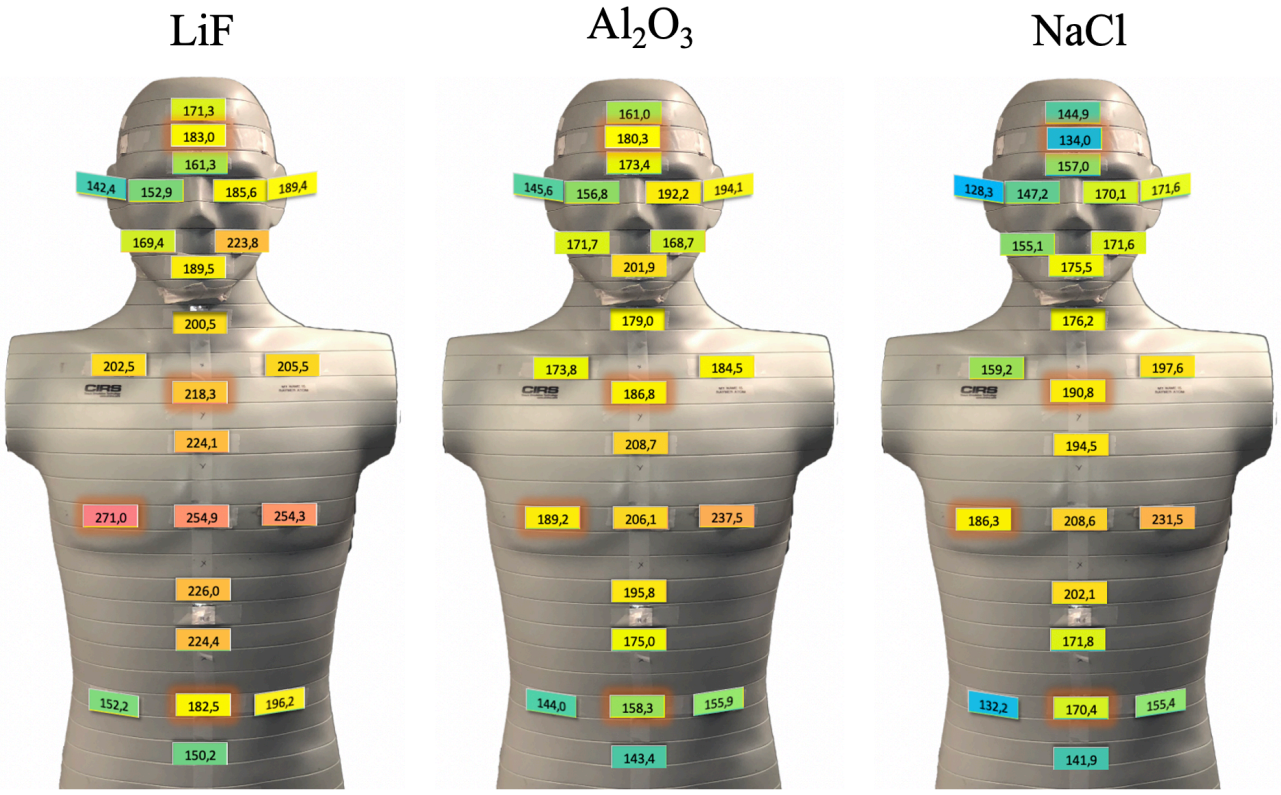


**Figure 24:** Estimated $D_w$ values (ranging from low-blue to high-red) for LiF, $Al_2O_3$ and NaCl, normalized to the total activity of the $^{137}Cs$ source (~0.75 GBq, t = 0) and total exposure time (96.4 h), [µGy $GBq^{-1}$ $h^{-1}$], for the laboratory measurement with activity uptake in the head.

The mean uncertainty for all $D_w$ values for the LiF is 15%, for the $Al_2O_3$ it is 12% and for the NaCl pellets it is 17%. The EPD at chest height, normalized to the total activity (~0.75 GBq) and exposure time (19 minutes), was 312 µSv $GBq^{-1}$ $h^{-1}$. For NaCl, the normalized dose value at chest height was 310.7 µSv $GBq^{-1}$ $h^{-1}$, in terms of $H_P(10)$. There is a 1% difference in the normalized $H_P(10)$ between the EPD and NaCl.

Figures 21-24 indicate that depending on which radiopharmaceutical is injected in the patient, different parts of the body turn into a temporary radiation source, emitting a complex radiation field depending on where all activity has been distributed. Hence, parts of the staff phantom that are closest to the patient phantom and specifically to the part from which the radiation field is emitted from, will receive the highest absorbed doses. In practice this has impact on how to best measure radiation exposure around different types of patients.

## 4.5 Clinical measurements

### 4.5.1 Difference in absorbed dose with and without lead apron during preparation and elution of radiopharmaceuticals

The following results are based on the assumption that all NM staff members work equally fast. Figure 25 shows estimated $D_w$ values normalized to the total activity of $^{99m}Tc$, [µGy GBq$^{-1}$], which was prepared in the hot lab during the time of the measurement, with (45.4 GBq) and without a lead apron (31.4 GBq), respectively. Considering 0.5 mm lead equivalence, close to 90% attenuation of the radiation is expected theoretically. In reality, the attenuation percentage is usually lower.

Comparing the signals visually for all three detector materials, it became apparent that the signals in the hot lab environment were low. The results for the $Al_2O_3$ discs are excluded, as the signals were below the detection limit. Thus, only results for LiF and NaCl are included.

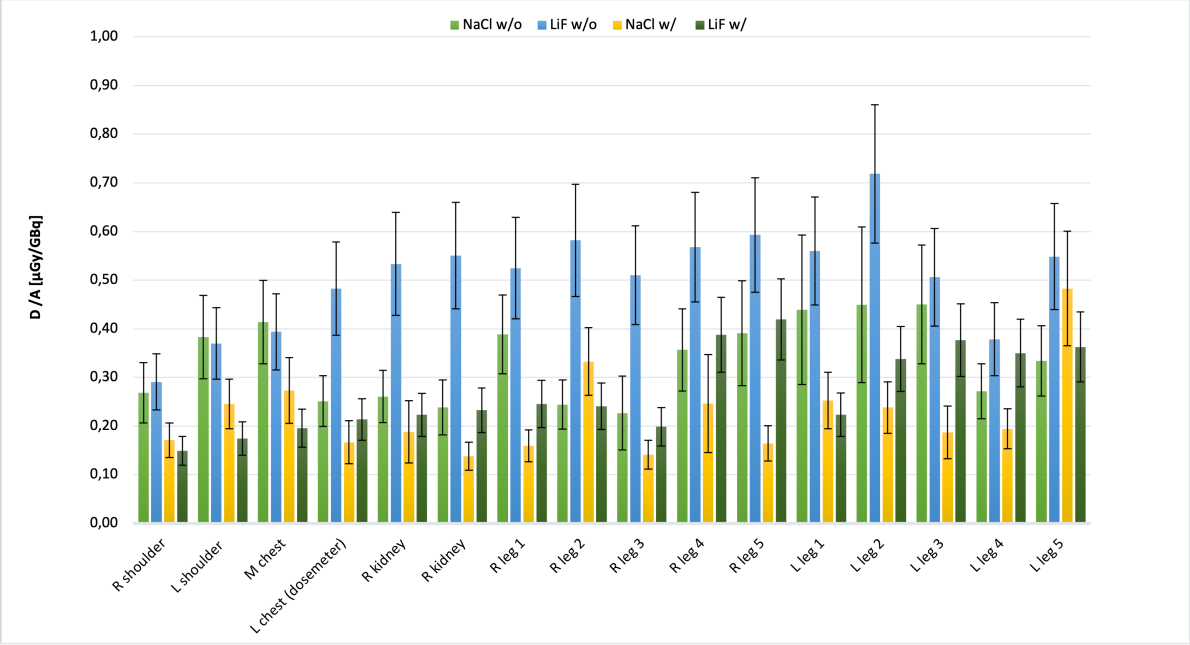


**Figure 25:** Estimated $D_w$ values normalized to the total activity of the prepared $^{99m}Tc$, for each measurement, with (45.5 GBq) and without (31.4 GBq) a lead apron, [µGy GBq$^{-1}$]. $D_w$ values are estimated for LiF and NaCl. Results were excluded for $Al_2O_3$ due to low signals in the clinic. The staples represent the estimations for dosemeter kits located on different parts of the torso and legs.

In Figure 25, the staples represent measured doses normalized to the handled activity for the dosemeter kits positioned on different parts of the body and the legs. The leg positions (named r-right and l-left from nr. 1-5), start from the thigh and move down.

The dosemeter kit positioned where the right kidney is located and the second position on the left leg, indicate higher dose values for NaCl, whereas for LiF this effect can barely be observed at the fourth position on the right leg. The differences between NaCl and LiF could be due to uncertainties in the energy dependencies or due to the low signals in the hot lab during the limited exposure time.

The NaCl pellets have a MDD of 6 µGy and a MMD of 20 µGy. The LiF chips have a detection threshold of 0.05 µGy, according to TLD Poland. The estimated $D_w$ values for both detector materials, during both measurements were above the MDD. However, due to the low signals in the hot lab environment, the estimated $D_w$ values were below the MMD for the NaCl pellets, which could potentially be one of the reasons why there is a significant difference in the dose- and signal response between NaCl and LiF with and without the lead apron. The results vary significantly from theoretical expectations. Based on the absolute dose values, there is an on average 31% difference with and without the lead apron for the NaCl and 46% difference for the LiF. The mean uncertainty for all $D_w$ values was estimated 20% for LiF and 25% for NaCl.

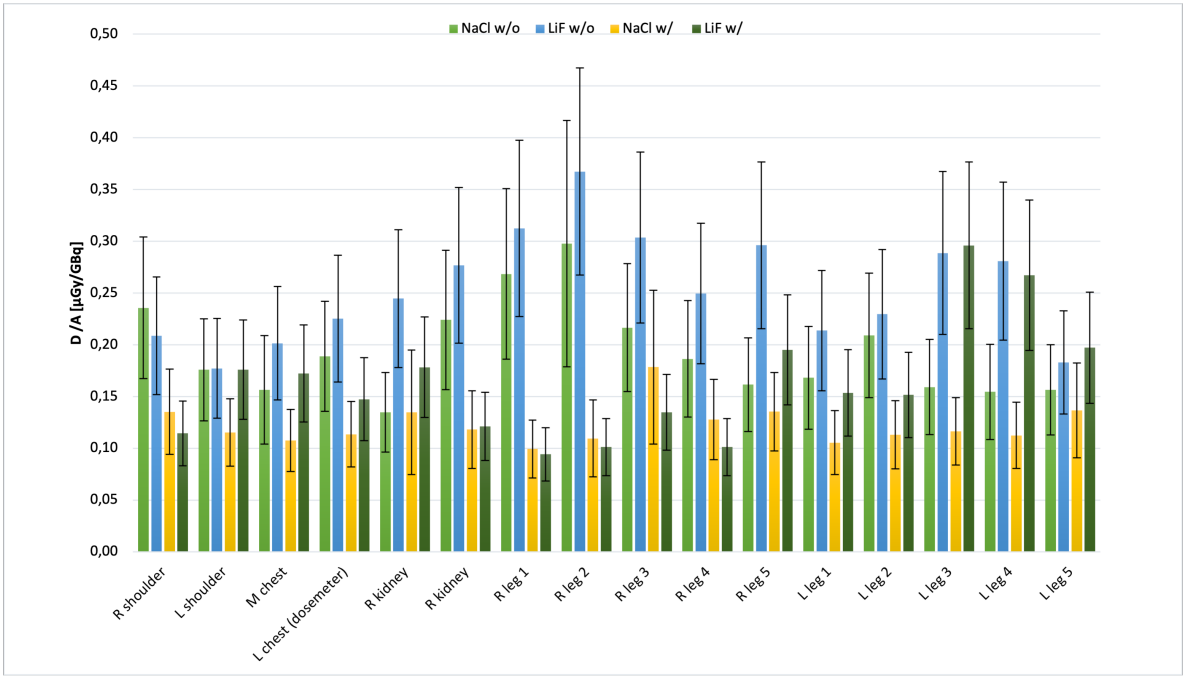


**Figure 26:** Estimated $D_w$ values normalized to the total activity of the eluted $^{99m}Tc$, for each measurement, with (83.8 GBq) and without (50.6 GBq) a lead apron, [µGy $GBq^{-1}$]. $D_w$ values are estimated for LiF and NaCl. Results were excluded for $Al_2O_3$ due to low signals in the clinic. The staples represent the estimations for dosemeter kits located on different parts of the torso and legs.

The same could be concluded from measurement during the elution of radiopharmaceuticals. LiF and NaCl measured absorbed doses at the same positions as in Figure 25. The $D_w$ values were normalized to the total activities, [µGy $GBq^{-1}$], of the elutions during one day, with (83.8 GBq) and without (50.6 GBq) a lead apron, and are shown in Figure 26. Hence, the normalized values show the dose distribution over the torso and the legs, as well as how well the estimations with LiF and NaCl agree with each other. The $D_w$ values for the two detector materials appear to be in agreement, on average within 25% with a lead apron and 15% without the lead apron. There is an on average 34% difference with and without the lead apron for the NaCl and 33% difference for the LiF. The mean uncertainty for all $D_w$ values in this measurement was estimated as 27% for LiF with and without a lead apron. For NaCl the mean uncertainty is 30% and 31%, with and without a lead apron, respectively.

Based on the dose estimations for both measurements (Figure 25 and Figure 26), the results indicate that a lead apron does help reduce the absorbed dose, although less than expected. The results also imply that the legs more or less receive a similar dose compared to other positions on the torso, which means the exposure from the ion chamber is insignificant. The results for the LiF chips in Figure 25 indicate more significant differences with and without the lead apron compared to the second measurement, and also compared to the results for NaCl in both measurements. One potential cause for the difference between measurements could be the difference in exposure time. The first measurement lasted for two days, whereas the second lasted one day.

### 4.5.2 Personal dosimetry for staff members at the nuclear medicine department at SUS Malmö

Table 2 presents the estimated personal dose equivalent, $H_P(10)$, and $D_w$ values to selected staff members of the NM department that wore the in-house developed dosemeters (dedicated for this project) together with their regular personal dosemeter (TLD) during one month. Results for the $Al_2O_3$ are excluded since the doses were below detection limits. In Table 2 it is indicated that the category B person (staff member 1 & 2), that only worked with $^{99m}Tc$, received a smaller dose compared to category A staff, which is expected considering the SSM directives on radiation protection for occupationally exposed personnel presented in section 2.5. The estimated dose values between the detector materials are in good agreement. Between the LiF chips in the in-house developed dosemeters and LiF chips in the regular personal TLDs, there is a factor 2 difference in the estimated dose values for staff member 1. However, this could be due to the difference in calibration units.

**Table 2:** Dose estimations for the in-house developed dosemeters worn by NM selected staff members for a time period of one month, along with their regular personal TLD. LiF and NaCl in the in-house developed dosemeters are calibrated in units of $D_w$ [mGy ± mGy]. NaCl is also calibrated in terms of $H_P(10)$ [mSv ± mSv], for comparison with the regular personal TLDs.

**In-house developed dosemeters [$D_w$ - mGy]**

| | Staff member 1 $^{99m}Tc$ | Staff member 2 $^{99m}Tc$ | Staff member 3 $^{18}F$ |
|---|---|---|---|
| **LiF** | 0.2 ± 0.02 | 0.1 ± 0.01 | 0.3 ± 0.03 |
| **NaCl** | 0.1 ± 0.01 | 0.1 ± 0.01 | 0.3 ± 0.04 |

**Regular personal dosemeter & NaCl [$H_p(10)$ - mSv]**

| | | | |
|---|---|---|---|
| **TLD** | 0.1 | 0.1 | 0.3 |
| **NaCl** | 0.1 ± 0.02 | 0.1 ± 0.02 | 0.4 ± 0.05 |

# 5. Conclusions

This project has shown that the absorbed dose estimations for the NaCl pellets and the other two commercial alternatives are in reasonably good agreement with each other. However, there are several uncertainties in the current comparisons that need to be taken into consideration and require further investigation, mainly the readout protocol for both LiF and $Al_2O_3$. The NaCl pellets have been extensively studied before. Thus, an optimized calibration protocol for the NaCl already exists. For this reason and in contrast to prior statements, when it was assumed that the LiF chips would be used as the most optimal reference for the other detector materials, it might be more reasonable to assume that the NaCl pellets will achieve more accurate dose estimations, considering the readout protocols for the LiF and $Al_2O_3$ are not optimized. However, this is hard to determine without an absolute reference. The LiF chips had not been used for approximately two years and require more time for calibration. These chips, as well as the $Al_2O_3$ discs are only used for research purposes. The $Al_2O_3$ discs came from discarded dosemeter holders, which means that there is a high probability for better dose estimations with new $Al_2O_3$ discs used with a dedicated readout protocol. For future works, it would be valuable to conduct more studies, comparing NaCl to other commercial alternatives at high, as well as low doses and dose rates and in different clinical applications.

On a similar note, the conversion factors, accounting for the difference in energy dependence and difference in units of calibration, which were used for the purpose of comparing all three detector materials, should also be further investigated. Conversion factors for NaCl, in terms of $H_P(10)$ or $D_{air}$, were predetermined in a previous project. In comparison, the conversion factors for the other two detector materials had to be estimated using mass energy-absorption coefficients, which is also true for NaCl, in terms of $D_w$. Thus, an uncertainty factor was included to account for the possible

effects of using mass energy-absorption coefficients, while not carefully examining the cavity theory.

Lastly, in reference to the NM staff members' curiosity regarding exposures near the disposal garbage bin and in the hot lab, the results from the clinical measurements indicated that the received absorbed doses were low. Figures 25-26 indicate that the lead apron does shield against radiation. The difference with and without a lead apron, can be deemed insignificant, considering the low signals in the clinic and the low absorbed doses. The dose estimations presented in this project showed acceptable estimations between the LiF chips and NaCl pellets. However, since the dose estimations for NaCl appeared below MMD, longer measurements are required in the clinic to accumulate enough signal to estimate proper absorbed dose values.

In order to be able to use NaCl as a personal dosemeter, it is also necessary to account for the potential changes in signal yield over time (i.e. inverse fading). Previous studies have shown that a potential solution is applying a mathematical correction factor. With a stable signal yield over time, it should be possible to achieve more accurate dose estimations. As previously mentioned, LiF and $Al_2O_3$ are used worldwide as a personal dosemeters. For LiF, one potential uncertainty that can also be regarded as a disadvantage is the heating of the material, which may affect the dosimetric properties over time.

To conclude, this project further confirms that the household salt (NaCl) has a strong potential to be utilized as an alternative point-and personal dosemeter in clinical applications.

# Acknowledgements

I would like to extend my sincere gratitude to my head supervisors, **Christian Bernhardsson & Lovisa Waldner,** for all their support and invaluable guidance throughout this project. I deeply appreciate the amount of devotion you both put into this project, which allowed me to learn and grow on a professional level. I also wish to thank the assisting supervisor, **Anniqa Rastbäck**, for your sincere commitment and encouragement. Your energetic and honest attitude made me feel comfortable and welcomed.

**Christopher Rääf**, a sincere thanks for sharing your insight with me during the OSL meetings and offering me helpful pieces of advice. **Mårten Dalaryd,** thank you for your help during my calibrations with the $^{60}$Co source at SUS Lund. Many thanks to **Sigrid Leide-Svegborn,** for all your help and insightful ideas concerning the NM clinic. Also, a special thanks to the volunteers at the NM department that helped me with my measurements.

I wish to thank everyone at the Medical Radiation Physics department at SUS Malmö for the warm welcome and delightful conversations. You made me feel calm and collected, and also made my time at SUS Malmö exceptionally enjoyable.

A sincere thanks to my fellow classmates, for all the encouragement during difficult periods and happy distractions during countless coffee breaks. Likewise, to all the teachers at MSF Malmö, thank you for everything you have taught us. These last three years have been wonderful.

Finally, I wish to dedicate my deepest gratitude to my loving family for believing in me and supporting me endlessly throughout my entire education. My accomplishments would mean nothing without you.

# References


Akselrod, M.S., Kortov, V.S., Kravetsky, D.J., Gotlib, V.I., 1990. Highly Sensitive Thermoluminescent Anion-Defective Alpha-Al203:C Single Crystal Detectors, Radiation Protection Dosimetry, 32(1), pp. 15–20, https://doi.org/10.1093/oxfordjournals.rpd.a080715.

Bailey, D.L., Humm, J.L., Todd-Pokropek, A., van Aswegen, A., 2015. Nuclear medicine physics, a handbook for teachers and students. Vienna. Nuclear Medicine Physics, INTERNATIONAL ATOMIC ENERGY AGENCY (IAEA), ISBN 978–92–0–143810–2.

Ben-Shachar, B., Weinstein, M., & German, U., 1999. LiF:Mg,Cu,P versus LiF:Mg,Ti: A comparison of Some dosimetric properties. Israel.

Bernhardsson, C., Christiansson, M., Mattsson, S. et al., 2009. Household salt as a retrospective dosemeter using optically stimulated luminescence. Radiat Environ Biophys, 48, pp. 21–28, https://doi.org/10.1007/s00411-008-0191-y.

Bos, A.J.J., 2001. High sensitivity thermoluminescence dosimetry. Nuclear Instruments and Methods in Physics Research Section B: Beam Interactions with Materials and Atoms, 184(1-2), pp. 3-28, ISSN 0168-583X. https://doi.org/10.1016/S0168-583X(01)00717-0.

Bøtter-Jensen, L., 2000. Development of optically stimulated luminescence techniques using natural minerals and ceramics, and their application to retrospective dosimetry, RISO-R—1211(EN), Denmark, ISBN 87-550-2756-3.

Christiansson M., 2014. Household salt as an emergency radiation dosemeter for retrospective dose assessments using optically stimulated luminescence, Doctor, Medical Radiation Physics, Malmö. ISBN 978-91-87651-51-9.

Christiansson, M., Bernhardsson, C., Geber-Bergstrand, T., Mattsson, S., Rääf, C.L., 2018. OSL in NaCl vs. TL in LiF for absorbed dose measurements and radiation quality assessment in the photon energy range 20 keV to 1.3 MeV. Radiation Measurements, 112, pp. 11-15, ISSN 1350-4487, https://doi.org/10.1016/j.radmeas.2018.03.003.

Currie, L.A., 1968. Limits for qualitative detection and quantitative determination. Application to radiochemistry. Anal. Chem. 40, pp. 586–593. https://doi.org/10.1021/ac60259a007.

DTU Nutech, Denmark, Center for nuclear technologies, 2017. Guide to The Risø TL/OSL Reader.

Ekendahl, D., Bulánek, B., Judas, L., 2016. A low-cost personal dosemeter based on optically stimulated luminescence (OSL) of common household salt (NaCl),Radiation Measurements, 85, pp. 93-98, ISSN 1350-4487. https://doi.org/10.1016/j.radmeas.2015.12.023.

Geber-Bergstrand, T., 2017. Optically Stimulated Luminescence for Retrospective Radiation Dosimetry. The Use of Materials Close to Man in Emergency Situations, Doctor, Department of Translational Medicine, Lund. ISBN 978-91-7619-460-7.

Hubbell, J.H., Seltzer S.M., 2004. Tables of X-Ray Mass Attenuation Coefficients and Mass Energy-Absorption Coefficients. National Institute of Standards and Technology (NIST), Gaithersburg, MD, Available at: https://www.nist.gov/pml/x-ray-mass-attenuation-coefficients,(Accessed: 2020-10-05)

Kortov, K., 2007. Materials for thermoluminescent dosimetry: Current status and future trends, Radiation Measurements, 42(4–5), pp. 576-581, ISSN 1350-4487, https://doi.org/10.1016/j.radmeas.2007.02.067.

Landauer, 2000. OSL TECHNOLOGY, OPTICALLY STIMULATED LUMINESCENCE, Available at: https://www.landauer-fr.com/en/knowledge/go-further/osl-technology/, (Accessed: 2020-12-12).

McKeever, S. W. S., Moscovitch, M., 2003. On the advantages and disadvantages of optically stimulated luminescence dosimetry and thermoluminescence dosimetry, Radiation Protection Dosimetry, 104(3), pp. 263–270, https://doi.org/10.1093/oxfordjournals.rpd.a006191.

TLD Poland, 2001-2005. LiF: Mg, Cu, P Thermoluminiscent phosphor and pellets. Available at: http://www.tld.com.pl/tld/index.html, (Accessed: 2021-03-25).

Nakajima,T., Murayama, Y., Matsuzawa, T., Koyano, A., 1978. Development of a new highly sensitive LiF thermoluminescence dosemeter and its applications, Nuclear Instruments and Methods, 157(1), pp. 155-162, ISSN 0029-554X, https://doi.org/10.1016/0029-554X(78)90601-8.

Poston, J.W., 2003. Dosimetry, Encyclopedia of Physical Science and Technology, Third Edition, Academic Press, pp. 603-650, ISBN 9780122274107, https://doi.org/10.1016/B0-12-227410-5/00185-X.

Pradhan, A.S., Lee, J. I., Kim, J. L., 2008. Recent developments of optically stimulated luminescence materials and techniques for radiation dosimetry and clinical applications. Journal of medical physics, 33(3), 85–99. https://doi.org/10.4103/0971-6203.42748.

SFS 2018:506. Strålskyddsförordning. Stockholm: Miljödepartementet. Available at: https://www.riksdagen.se/sv/dokument-lagar/dokument/svensk-forfattningssamling/stralskyddsforordning-2018506_sfs-2018-506, (Accessed: 2021-03-23)

Sharp, P.F., Gemmell, H.G., Murray, A.D., 2005. Practical Nuclear Medicine. Third edition, London, Springer-Verlag.

SSMFS 2018:1. Strålsäkerhetsmyndighetens föreskrifter om grundläggande bestämmelser för tillståndspliktig verksamhet med joniserande strålning. Stockholm: Strålsäkerhetsmyndigheten (SSM). Available at: https://www.stralsakerhetsmyndigheten.se/publikationer/foreskrifter/ssmfs-2018/ssmfs-20181/, (Accessed: 2021-01-05)

Sylvain, I., Bernard, B., 2002. Radiation exposure in nuclear medicine: real-time measurement. Brazilian Archives of Biology and Technology. 45. pp. 111-114. ISSN 1516-8913

Thomsen, K.J., 2004. Optically stimulated luminescence techniques in retrospective dosimetry using single grains of quartz extracted from unheated materials. Risø National Laboratory. Risø-PhD, (1)

Vargas, C.S.,Vanhavere, F., 2011. Optically Stimulated Luminescence dosimetry using Al2O3:C micro crystals. Limoges, France: UL - Université de Limoges.

Waldner, L., 2017. NaCl pellets for improved dosimetry. Department of medical radiation physics, clinical sciences, Lund, Lund University.

Waldner, L., Bernhardsson, C., 2018. Physical and dosimetric properties of NaCl pellets made in-house for the use in prospective optically stimulated luminescence dosimetry applications. Radiation Measurements, 119, pp. 52-57, ISSN 1350-4487, https://doi.org/10.1016/j.radmeas.2018.09.001.

Waldner, L., Rääf, C. & Bernhardsson, C., 2020. NaCl pellets for prospective dosimetry using optically stimulated luminescence: Signal integrity and long-term versus short-term exposure. Radiat Environ Biophys, 59, pp. 693–702. ISSN 0301-634X. https://doi.org/10.1007/s00411-020-00873-8.

Yukihara, E.G., Mckeever, S.W.S., 2011. Optically Stimulated Luminescence. John Wiley & Sons Ltd.